

A High-Throughput and Genomics-Based Approach to Combat Antimicrobial Resistance

Michael Mahdavi

A Thesis in
The Department of
Chemistry and Biochemistry

Presented in Partial Fulfillment of the Requirements
For the Degree of Master of Science (Biochemistry) at
Concordia University
Montréal, Québec, Canada

December 2022

© Michael Mahdavi, 2022

CONCORDIA UNIVERSITY
School of Graduate Studies

This is to certify that the thesis prepared

By: Michael Mahdavi

Entitled: A High-Throughput and Genomics-Based Approach to
Combat Antimicrobial Resistance

and submitted in partial fulfillment of the requirements for the degree of

Master of Science (Biochemistry)

complies with the regulations of the University and meets the accepted standards
with respect to originality and quality.

Signed by the final examining committee:

_____ Chair
Dr. Xianming Zhang

_____ Examiner
Dr. Peter Pawelek

_____ Examiner
Dr. Steve Shih

_____ Thesis Supervisor(s)
Dr. Brandon Findlay

Approved by _____

Dr. Louis Cuccia (Graduate Program Director,
department of Chemistry)

January 13, 2023

Pascale Sicotte (Dean of Arts & Science)

Abstract

A High-Throughput and Genomics-Based Approach to Combat Antimicrobial Resistance

Michael Mahdavi

Antimicrobial resistance (AMR) is becoming an increasingly large threat to global health and economics. In 2019, there were approximately 1.27 million deaths directly attributable to bacterial AMR and 4.95 million deaths associated with bacterial AMR. These numbers are expected to increase to 10 million by the year 2050. The use of Adjuvant therapeutics has been proposed as a strategy to mitigate antimicrobial resistance. Adjuvants can help resensitize resistant bacteria to clinically-relevant antibiotics, while also prolonging resistance from occurring.

Here I present two high-throughput screens: one that identifies robust adjuvant compounds that target resistant bacteria, and one that repurposes drug-like compounds for antimicrobial use against Gram-negative bacteria. From these screens, one lead adjuvant candidate and four repurposed drug-like antimicrobials were taken forward for a mix of analog generation studies, mechanistic studies, resistance evolution studies and genomic analysis.

This work will help play a role in bringing novel therapies to the clinic and prolong the evolution of resistance from occurring.

Acknowledgements

Thank you to my supervisor, Dr. Brandon Findlay, for his continued guidance and support throughout my Master's. Thank you for believing in me and supporting me to explore my passions. Dr. Findlay has been a great mentor and I've learned so much from him throughout my Master's. I'd like to give a special thanks to Laura Domínguez, my best friend, my lab mate, and my partner, who has helped me greatly throughout my degree. She has always been there for me, listening to my ideas, offering her valuable insights and providing emotional support during the challenging times. Her belief in me and my abilities has kept me motivated and inspired me to work hard and achieve my goals. Laura has supported me in several ways including, preparing for committee meetings and presentations, helping in the lab with experiments, editing figures, proofreading my thesis, and encouraging me at every step. I truly couldn't have done it without her. Thank you to my lab mates, Laura Domínguez, Liana Zaroubi, Bahar Pakseresht, Lydia Rili, Prerna Singh, Farhan Chowdhury, Dr. Md Ali Yousof, and Ryan Dupuis for creating a great work environment filled with support, laughter, and fun. I'd like to thank my colleagues, Nadia Sari, Maxwell Miller, and Nour Ghaddar for their previous work in the lab that helped shape my project. It was an honour to be a part of the Findlay Lab.

I'd like to express my gratitude to my committee members, Dr. Peter Pawelek and Dr. Mike Hallett for their guidance and feedback throughout my degree. I'd like to thank the Department of Chemistry at Concordia University for providing me with the resources to achieve my Master's. I'd like to thank the Fonds de Recherche du Québec – Santé for funding

and supporting this research project. Finally, I'd like to thank my collaborators, Dr. Dustin Duncan, Dr. Karine Auclair, Phil Prevost, and Dr. Pat Forgione for their effort in pushing our research forward.

Contributions of Authors

Shown below are the contributions of each of the authors in this thesis.

Michael Mahdavi: Wrote the first draft of this thesis and corrected subsequent versions. Performed all listed experiments and analyses.

Dr. Brandon Findlay: Project supervisor responsible for correcting this thesis.

Laura Domínguez: Proofreading and editing this thesis.

Nadia Sari: Collected, sequenced, and performed early NGS analysis of the bacterial samples for the bacterio-modulation project.

Maxwell Miller: Collected and established protocol for bacterial samples for the bacterio-modulation project.

Nour Ghaddar: Generating resistant *E. coli* cells.

Phil Prevost: Generating analogs for the lead candidates of the Pathogen Box project.

Dr. Dustin Duncan: Synthesizing and providing 3NP for bacterio-modulation studies. Generating the early data for which this project was based on.

Marcos Di Falco: Performed high-resolution liquid chromatography-mass spectrometry on the Pathogen Box compounds.

C³G and Genome Quebec: Sequenced and analyzed our bacterio-modulation bacterial samples.

Copyright Information

Parts of this thesis are adapted from a manuscript currently in preparation for submission.

Table of Contents

List of Figures	ix
List of Tables	x
List of Abbreviations	xi
INTRODUCTION.....	1
<i>Bacterial resistance mechanisms</i>	1
<i>Antibiotic adjuvant strategies</i>	6
<i>Gradient evolution chambers</i>	10
<i>High-throughput screening for adjuvant discovery</i>	12
<i>Exploring adjuvant mechanism of action</i>	15
<i>Repurposing drug-like compounds for antimicrobial use</i>	18
<i>Bacterio-modulation genomics analysis</i>	20
Materials & Methods:.....	26
<i>Chemicals and Plasticware:</i>	26
<i>Natural product library:</i>	26
<i>Strains</i>	27
<i>M9A+ media:</i>	28
<i>Evolution of antibiotic resistance:</i>	29
<i>Generation of speed-selected E. coli strains</i>	30
<i>Generation of clonal and population samples</i>	31
<i>Illumina shotgun sequencing:</i>	31
<i>Antibiotic Susceptibility Testing</i>	32
<i>High-throughput screen for adjuvants</i>	33
<i>High-throughput screen of Pathogen Box compounds</i>	33
<i>Pathogen box quality control</i>	34
<i>Checkerboard assays</i>	35
<i>Membrane depolarization assay</i>	36
RESULTS:	37
<i>The primary screen</i>	37
<i>Perforone allows protons to flow across the membrane</i>	47

<i>Pathogen Box Screen:</i>	50
<i>Bacterio-modulation genomic analysis:</i>	53
Discussion:	58
References	66

List of Figures

Figure 1: Preparation of SAGE plates.....	12
Figure 2: Distribution of therapeutic indications of the pathogen box compounds.....	18
Figure 4: Schematic showing the tricarboxylic acid (TCA) cycle, glyoxylate shunt, and ITA degradation pathway.....	21
Figure 5: Structure of 3-nitro-pantothenate (3NP).	21
Figure 6: Illumina sequencing workflow.	23
Figure 7: Checkerboard layout.....	35
Figure 8: Adjuvant discovery pipeline.....	37
Figure 9: Hit candidates from the primary screen.....	41
Figure 10: Validation screen of library of natural products using PMBN	42
Figure 11: Primary screen activity profile of the 6 selected candidates.	43
Figure 12: Synergy between doxycycline and adjuvant candidates against doxycycline-resistant <i>E. coli</i> cells checkerboard assays.....	43
Figure 13: Synergy between Polymyxin and adjuvant candidates against polymyxin-resistant <i>E. coli</i> cells.....	43
Figure 14: Synergy between polymyxin and adjuvant candidates against polymyxin-resistant <i>E. coli</i> cells.....	43
Figure 15: Synergy between azithromycin and adjuvant candidates against azithromycin-resistant <i>E. coli</i> cells.....	44
Figure 16: Synergy between ciprofloxacin and adjuvant candidates against ciprofloxacin-resistant <i>E. coli</i> cells.....	44
Figure 17: Synergy between trimethoprim/ sulfamethoxazole and adjuvant candidates against trimethoprim/sulfamethoxazole-resistant <i>E. coli</i> cells.....	44
Figure 18: Structure of perforone.....	46
Figure 19: i) Synergy between perforone and polymyxin against naïve <i>E. coli</i>	46
Figure 20: Synergy between perforone and melittin against <i>S. aureus</i> ATCC 29213.....	47
Figure 21: Measuring changes in transmembrane potential using DiSC ₃ (5).....	49
Figure 22: Measuring <i>E. coli</i> MG1655 cytosolic pH with BCECF, AM.. ..	49
Figure 23: Pathogen Box lead candidates.....	50
Figure 24: SNPs found in population samples.	55
Figure 25: SNPs found in clonal samples.	56
Figure 26: i) 3NP + ITA-naïve <i>S. Typhimurium</i> checkerboard.....	57

List of Tables

Table 1: Bacterial strains and suppliers.	27
Table 2: M9A+ ingredients.	28
Table 3: Samples sent for Illumina shotgun sequencing	32
Table 4: MICs of naïve and resistant MG1655 <i>E. coli</i> cells.	38
Table 5: Summary of Pathogen Box screen.	49
Table 6: Activity of generated analogs of compound 11.	53

List of Abbreviations

- AMR Antimicrobial Resistance
- HGT Horizontal Gene Transfer
- DNA Deoxyribonucleic acid
- LPS Lipopolysaccharides
- SNP Single Nucleotide Polymorphisms
- PBP Penicillin-binding proteins
- MRSA Methicillin-resistant *Staphylococcus aureus*
- HTS High Throughput Screen
- MIC Minimum Inhibitory Concentration
- OD Optical Density
- FIC Fractional Inhibitory Concentration
- FME Fractional Maximal Effect
- EDTA Ethylenediaminetetraacetic acid
- ITA Itaconic Acid
- 3NP 3-nitro-pantothenate
- Ict Itaconate coenzyme A transferase
- Ich Itaconyl-CoA hydratase
- Ccl (S)-citramalyl-CoA lyase
- NGS Next Generation Sequencing
- DiSc₃(5) 3,3'-Dipropylthiadiazocyanine Iodide
- BCECF, AM Ester 2',7'-Bis-(2-Carboxyethyl)-5-(and-6)-Carboxyfluorescein, Acetoxymethyl Ester
- MMV Medicines for Malaria Venture
- CAMHB Cation-Adjusted Mueller–Hinton Broth
- SS Speed Selected
- CAMHA Cation-Adjusted Mueller–Hinton Agar
- DMSO Dimethyl sulfoxide
- FIC Fractional Inhibitory Concentration
- GC Growth Control
- SC Sterility Control
- EGFR Epidermal Growth Factor Receptor
- CAIX Carbonic anhydrase IX
- PG Phosphatidylglycerol
- PaβN Phenylalanine-arginine-β-naphthylamide
- MRG Macrolide resistance genes
- DHFR Dihydrofolate reductase
- QRDR Quinolone resistance determining region
- tRNA Transfer RNA
- rRNA: Ribosomal RNA

INTRODUCTION

Antimicrobial resistance (AMR) is becoming a major threat to global health. In 2019, there were approximately 1.27 million deaths directly attributable to bacterial AMR and 4.95 million deaths associated with bacterial AMR¹. Some have speculated that if left unchecked, antibiotic-resistant bacteria these numbers will increase to 10 million per year by 2050². The discovery and use of antibiotics was a pivotal moment in medicine, allowing us to mitigate microbial infections³. But, driven by a combination of chromosomal mutations and horizontally transferred resistance elements, resistance has been observed against every antibiotic in current clinical use. For example, resistance against ampicillin was observed in 1940, two years prior to it being introduced into the clinic^{4,5}.

The rising prevalence of resistance is a natural consequence of antibiotic use, which imposes a selective pressure on pathogenic bacteria⁶. Evolution of resistance over the course of an infection can compromise therapy, and in the case of the developmental candidate AN3365/GSK2251052, even forced an abrupt halt to a phase II clinical trial⁷. As the development of new drugs has not kept pace with bacterial evolution⁸, methods to restore the efficacy of existing antibiotics are urgently required.

Bacterial resistance mechanisms

Naïve bacteria can become resistant to antibiotics through horizontal gene transfer (HGT) and spontaneous mutations, allowing them to gain resistance through limiting drug uptake, modifying a drug target, inactivating the drug, or effluxing the drug out of the cell⁹. HGT is the process of bacteria obtaining foreign DNA from the environment. This can occur through transformation, conjugation and transduction¹⁰. Plasmid-mediated resistance involves the transfer of antibiotic resistance genes through a plasmid carrier. These plasmids are transferred between bacteria from either the same or different species. These genes encode for proteins that allow the bacteria to overcome the antibiotic's mode of action¹¹.

Alternatively, spontaneous mutations occur during cellular replication causing mutations in the bacterial genome. In some cases, these mutations can alter genes and overall cellular function, which allows the bacteria to overcome the antibiotic. Bacterial tuning of mutation rates has also been observed upon antibiotic stress, where the activation of stress responses allows for a transient increase of the mutation rates. This allows for rapid adaptation to new environments^{12,13}.

Single nucleotide polymorphisms (SNPs) are a type of mutation, where we observe single base pair variations in the genome¹⁴. At the genetic level, resistance can be seen from the SNPs in genes linked to antibiotic uptake, action, or efflux. SNPs can fall within the coding, non-coding, or intergenic regions of these genes. SNPs in the coding regions of genes can be split up between synonymous and nonsynonymous mutations. Synonymous mutations do not alter the amino acids, but are still able to alter the structure, function, and expression level of

proteins, affecting messenger RNA splicing and stability as well as protein folding¹⁵.

Nonsynonymous mutations can be further broken down into missense SNPs, a single nucleotide change which results in a change in protein sequence, and nonsense SNPs, a point mutation changing to a stop codon and resulting in a non-functional protein. Mutations that ultimately alter the function of a specific gene/protein may contribute to resistance¹⁶.

There are several types of antibiotic classes such as polymyxins, beta-lactams, aminoglycosides, tetracyclines, macrolides, quinolones, and sulfonamides¹⁷. Resistance against these antibiotic classes can occur in several ways, but tend to be related to the mechanism of action of the antibiotic¹⁷. For example, from the polymyxins class, polymyxin B is a polypeptide that has a bactericidal effect on Gram-negative bacilli¹⁸. This positively charged compound displaces the Ca^{+2} and Mg^{+2} ions that stabilize lipopolysaccharides (LPS) on the outer membrane¹⁸. This results in pore formation and the leakage of cytoplasmic content which eventually results in cell death¹⁹. Therefore, resistance to polymyxin occurs primarily by modifications to the LPS, through chromosomal mutations that result in the addition of 4-amino-4-deoxy-L-arabinose (arnB gene) and/or phosphoethanolamine (pmrCAB operon) to a phosphate group of the lipid A moiety of LPS^{20,21}. This addition reduces the affinity of cationic molecules, such as polymyxin and results in resistance to the drug¹⁸.

Azithromycin is part of the macrolide antibiotic class, effective against Gram-positive and Gram-negative bacteria²². It binds to the 23S rRNA in the 50S ribosomal subunit, at the exit site of the nascent peptide and thus inhibiting protein synthesis²³. There have been genes

described as macrolide resistance genes (MRG), such as macrolide efflux pumps encoded by the *msr(A)*, *mef(A)* or *mef(B)* genes²². Another resistance mechanism involves altering the drug target, observed by modifications in the *rrl* genes or in the presence of *erm*²³. This prevents the drug from binding to the 23S target²³.

Trimethoprim and sulfamethoxazole act synergistically by inhibiting different steps in the synthesis of folic acid²⁴. Sulfamethoxazole inhibits the enzyme dihydropteroate synthetase (DHPS), while trimethoprim inhibits dihydrofolate reductase (DHFR), catalyzing a successive step in the pathway²⁴. This drug combination is bacteriostatic as folic acid is a necessary precursor for protein and nucleic acid synthesis²⁴. Some resistance mechanisms observed have been mutations in either the promoter or coding regions of the *dhfr* gene, with notable prevalence of transferable resistance genes to trimethoprim from the variants *dhfrI* and *dhfrII*²⁴. Changes in *folP* have also been recorded to provide resistance to sulfamethoxazole by changing the tertiary structure of the DHPS enzyme²⁴.

Ciprofloxacin is a bactericidal drug part of the fluoroquinolone drug class²⁵. It can inhibit two topoisomerase II enzymes, DNA gyrase and DNA topoisomerase IV, both involved in relaxing the DNA supercoiling induced during replication of DNA²⁵. Resistance to this drug occurs through changes in the *gyrA/gyrB* genes, coding for DNA gyrase or *parC/parE* which code for topoisomerase IV²⁶. Together, these four genes are designated the “Quinolone-resistance determining region” (QRDR)²⁶. Resistance can also be achieved through efflux of the drug²⁵.

Part of the tetracyclines, doxycycline is a broad-spectrum antibiotic effective against both Gram-positive and Gram-negative bacteria²⁷. It is usually regarded as a bacteriostatic antibiotic, but this observation is strain dependent²⁷. Their mechanism of action is inhibition of protein synthesis by binding to the 16S rRNA in the 30S subunit of the bacterial ribosome²⁷. This inhibits the tRNA from docking during elongation. Tetracycline passively diffuses through the *ompC* and *ompF* porins²⁷. Resistance to doxycycline has been achieved mainly by genetic modifications to the genes encoding for the rRNA target²⁷. Such is the case for deletions or mutations in the *rpsJ* gene which corresponds to residues 53 to 60 of the gene encoding for the 30S subunit²⁷. Another mechanism of resistance is the expression of tetracycline ribosomal protection proteins (RPP) that are usually encountered in mobile genetic elements (MGE)²⁷. Examples of these proteins are Tet(O) and Tet(M), which enable ribosomal dissociation in a GTP dependent reaction. Efflux and tetracycline modifying enzymes have also been reported²⁷.

On the other hand, some bacteria are intrinsically resistant through their inherent properties which allows them to be resistant to specific antibiotics independent of horizontal gene transfer or prior exposure to antibiotics. For example, mycobacteria possess membranes with higher lipid content, this increased hydrophobicity will inherently make the cells less susceptible to non-polar drugs (like rifampicin or fluoroquinolones), whereas the opposite would be true for hydrophilic drugs²⁸. Another example of intrinsic resistance can be seen with *Listeria monocytogenes* and cephalosporins. Cephalosporins are beta-lactam antibiotics which inhibit cell wall synthesis in bacteria²⁹. They do this by binding to penicillin-binding proteins

(PBPs) preventing them from cross-linking peptidoglycan²⁹. The cell can no longer link together the nascent peptidoglycan chains after the existing peptidoglycan is degraded which leads to cell death²⁹. *L. monocytogenes* possess different PBPs such as PBP B3, encoded by the Imo0441 gene, and PBP 2A, that aren't inhibited by cephalosporins due to poor binding^{30,31}.

Gram-negative bacteria are notoriously more difficult to eradicate than Gram-negative bacteria due to differences in cell membranes³². Gram-positive bacteria possess a single-layered membrane composed of peptidoglycan, while Gram-negative bacteria have a double-layered membrane composed of peptidoglycan and lipopolysaccharide (LPS) outer membrane³². As a result of the double-layered membrane, Gram-negative bacteria are more difficult to target with drugs, as some compounds cannot pass through the membrane and enter the cell³³. Compounds that are able to cross the membrane of Gram-negative bacteria and enter the cell typically enter through narrow porins which are composed of Beta-barrel proteins. However, once inside the cell, bacterial efflux pumps will pump them out of the cell so compounds must accumulate faster than they are pumped out³⁴.

Antibiotic adjuvant strategies

The current panel of clinical antibiotics is effective against naïve or regular-functioning cells³⁵. However, these antibiotics will be ineffective against the bacteria if they gain resistance. For example, if a resistant bacteria has acquired a mutation that modifies an outer membrane antibiotic-binding receptor, then the antibiotic will no longer be able to bind and effectively kill the bacteria³⁶. In the clinical setting, this will allow resistant bacteria to persist and the infection

to worsen. One approach to mitigate this is to identify therapeutics that specifically target and eradicate resistant cells³⁷. This therapeutic could be used in combination with traditional antibiotics to target both naïve cells and resistant cells. This is applicable in the clinical setting since bacterial infections are often composed of both naïve and resistant bacteria^{38,39,40}.

Although developing antibiotics that specifically target resistant cells is a step in the right direction, resistance will eventually emerge against these new compounds since they are still imposing a selective pressure against the bacteria. This is evident in methicillin-resistant *Staphylococcus aureus* (MRSA) and other “super bugs” which gain resistance to several antibiotics and mechanisms of actions over time.^{41,42} This is why this method should be paired with the use of adjuvants. These compounds possess little to no antimicrobial activity against bacteria but are able to synergize with and enhance antibiotic function or restore activity against resistant strains. Since adjuvants have little to no antimicrobial activity on their own, there will be less genetic selection against them, thus prolonging resistance from occurring⁴³.

For example, in the case where bacteria gain resistance against a potent antibiotic, the MIC of the antibiotic increases. By using an adjuvant that enhances the activity of the antibiotic to function against resistant bacteria, one is decreasing the MIC of the antibiotic against resistant cells, which selects for naïve cells, allowing them to outcompete the resistant cells. Naïve cells can be better controlled in a clinical setting through the use of existing antibiotics⁴⁴.

Adjuvants can synergize with antibiotics in several ways by enhancing antibiotic accumulation, inhibition of signalling pathways and regulatory pathways related to antibiotic resistance, enhancing host defense, and inhibiting enzymes inhibiting enzymes⁴⁵.

Adjuvants can help antibiotics accumulate in the bacterial cell by facilitating the antibiotic across the outer membrane. An example of this is the two-peptide bacteriocin, PLNC8 $\alpha\beta$ ⁴⁶. Through growth inhibition studies, membrane permeability assays, and microscopy, PLNC8 $\alpha\beta$ was found to be effective in permeabilizing the bacterial membrane. It was able to synergize with many antibiotics such as, vancomycin, rifampicin, gentamicin, and, teicoplanin, to lower their MIC⁴⁶.

Adjuvants can also act as efflux pump inhibitors to help with antibiotic accumulation. The chemical family, pyranopyridines, were found to be robust efflux pump inhibitors through acting as substrate binders⁴⁷. They can preferentially bind to the efflux pump, instead of the antibiotic. MBX2319 is a novel pyranopyridine efflux pump inhibitors with potent activity against RND efflux pumps, specifically, AcrB⁴⁷.

Adjuvants can act to destroy biofilms or inhibit their formation, which allow the antibiotic to gain access to the cells where it can function. The class of small molecules, 2-aminoimidazoles, has been found to inhibit and disperse biofilms across a wide range of bacteria⁴⁸. An aminoimidazole/triazole conjugate showed synergy in combination with antibiotics, and was able to eradicate and disperse biofilms of MRSA and multidrug-resistant

Acinetobacter baumannii (MRAB)⁴⁸. This conjugate was later found to function through collapsing both components of the mycobacterial PMF ($\Delta\psi$ and ΔpH) and interferes with the electron transport chain⁴⁸.

Lastly, adjuvants can enhance the host defence by stimulating immune cells such as macrophages⁴⁴. One study identified streptazolin through a screen of microbial natural product extraction as an enhancer of macrophage killing activity against *Streptococcus mutans*⁴⁹. It was found that streptazolin stimulated macrophage activity through the phosphoinositide 3-kinase pathway resulting in upregulation of nuclear factor- κB ⁴⁹.

Adjuvants can inhibit antibiotic-degrading enzymes which allow the antibiotic to persist and function on the bacteria. For example, an adjuvant could function as a beta-lactamase inhibitor, which restores the activity of beta-lactam antibiotics⁴⁴. The beta-lactamase inhibitor, clavulanic acid, is one such adjuvant, effective against Ambler class A beta-lactamases. As a combination therapy with beta-lactam amoxicillin, clavulanic acid is on the World Health Organization's list of essential medications, with over six million prescriptions each year in the United States⁵⁰. However, as all antimicrobial agents do, resistance against amoxicillin-clavulanic acid emerged in the clinical setting over time⁵¹. One study reported on the incidence and mechanisms of amoxicillin-clavulanic acid-resistant *E. coli* in the clinical setting. It was found that the predominant mechanism for resistance was the overproduction of OXA-1 and other beta-lactamases, which are less sensitive to inhibition by clavulanic acid⁵².

Gradient evolution chambers

In the past, labour-intensive sub-culturing techniques needed to be employed in order to generate resistant bacteria⁵³. Recent advancements such as morbidostats and Microbial Evolution and Growth Arena (MEGA) plates have allowed researchers to map the genotypic pathways of antibiotic resistance^{54,55}. A morbidostat is an automated fluidic system which continuously measures the growth rates of evolving microbial populations and adjust antibiotic concentrations in the system to maintain a constant inhibition^{54,56}. The morbidostat is constructed using multiple pump arrays, tube arrays, glass vials, and media reservoirs. In liquid environments, resistant mutants tend to be less fit and are difficult to obtain since they are a small percentage of the population until the antibiotic eradicates the susceptible strains.⁵⁷ MEGA plates are large antibiotic evolution chambers(120 × 60 cm) used for the generation of bacteria that are greatly resistant to the antibiotics they are trialed with ($\approx 20,000x$ the initial MIC). These desk-sized MEGA plates are large in size so the operational throughput is limited. As described above, these techniques have complex setups so they are not accessible to many research labs⁵⁵. The soft agar gradient evolution (SAGE) plate system is a technique that is more high throughput and less labour-intensive and costly.

As seen in Figure 1, SAGE plates are constructed using regular lab equipment such as culture dishes, pipettes and media so the setup is relatively simple. Several plates can be run in parallel in a high-throughput manner. An antibiotic gradient is created throughout the plate and bacteria are inoculated on the side of the plate with the least amount of antibiotic and incubated. The bacteria will preferentially swim across the plate into increasing amounts of

antibiotics in order to scavenge for untapped nutrients⁵⁸. This is due to chemotaxis, the movement of a microorganism in response to a chemical stimulus. As the bacteria swim across the plate and encounter more antibiotic stress, selection events and random mutations occur, allowing the bacteria to gain resistance and continue consuming and traversing to the end of the plate. The antibiotic subjects the bacteria to a selective pressure which causes the mutation rate to increase, therefore allowing resistance-conferring mutations to arise^{13,12}.

Mutations that result in substantial increases to the MIC are likely to arise in the clinic. For screening purposes, the SAGE plate is an effective system to generate resistant cells that possess these types of high-impact mutations⁵⁹. Through one run, the SAGE plate can potentially generate resistant bacteria that possess a multifold increase in MIC against an antibiotic. The MIC can be further increased by sampling the resistant bacteria from the end of the plate and propagating them to another SAGE plate with a higher antibiotic gradient. In addition to this, mutations can be tracked over time as the bacteria swim across the plate. Analyzing these SNPs can reveal novel insights on the emergence of antimicrobial resistance. For example, one can learn about which resistance mechanisms tend to occur in the bacteria during 10X the MIC vs 50X the MIC of an antibiotic. As in nature, SNPs are the most commonly found form of mutation in the clinic, since they tend to be the simplest⁶⁰. For example, under stress a bacterial polymerase may select the wrong nucleotide, thereby changing the gene function⁶¹. The SAGE plate is also useful for analyzing mutations that occur over time and over the antibiotic gradient.

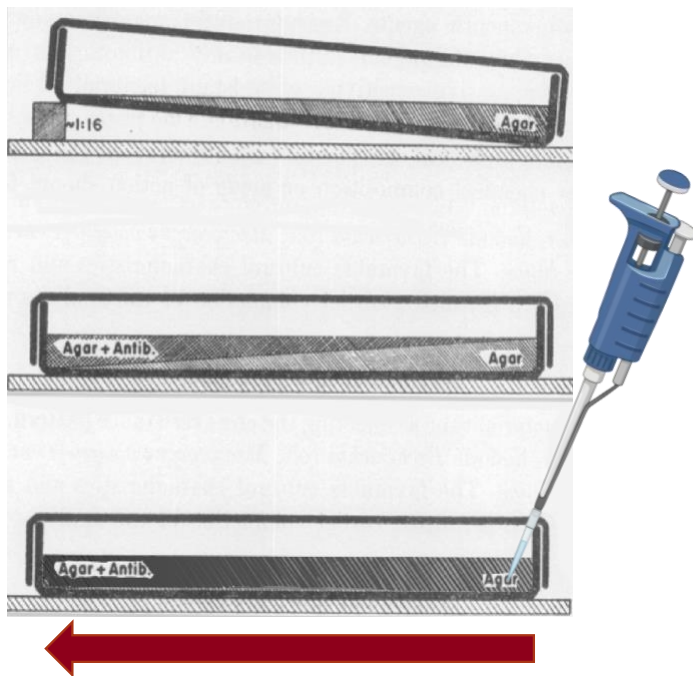


Figure 1: Preparation of SAGE plates. Arrow is indicating the direction of increasing antibiotic concentration (adapted from Szybalski, et al., 1952)⁶².

High-throughput screening for adjuvant discovery

Most antibiotics ($\approx 75\%$) are discovered and sourced from natural products that are produced by microorganisms⁴⁷. Synthetic compounds have also been used as antibiotics and are usually based on natural product chemical structures as a reference⁴⁸. Bacterial natural products function in several ways in nature such as communication between bacteria¹, decomposition of matter for nutrients¹, predation and defence¹, and as a warning signal¹. Adjuvant compounds can also be sourced from natural products. For example, clavulanic acid is produced by *Streptomyces clavuligerus*¹. One study strove to find an efflux pump inhibitor adjuvant molecule that is specific to the MacAB pump¹. Through a natural product library screen, they were able to identify OU33858 (5-[(5-chloro-2-hydroxyphenyl) methylene]-3-propyl-2-thioxo-1,3-diazolidin-4-one) as an efflux pump inhibitor with adjuvant-like activity.

This was a useful study to reference as it showed that adjuvants could be identified through a natural product screen and that screening against an efflux pump or other resistant-conferring targets is a promising approach.

High-throughput screening (HTS) is an effective drug discovery approach to screen large libraries and generate lead candidates that fit a criteria.^{63,64} The screen setup can be very broad depending on what the researcher is trying to find/measure. HTS has been possible due to advances in lab techniques, hardware and software. For example, the microtiter plate reader has allowed researchers to rapidly test a large number of samples and quantitatively measure experimental outputs such as optical density and fluorescence.⁶⁵ Automation tools, such as robotics, has removed the burden of repetitive manual labour, while also minimizing error and increasing throughput.⁶⁶ Many variables can be measured for screening such as enzyme inhibition, bacterial growth and death, receptor binding, etc.

In a HTS, the primary screen serves as a first pass of the library to identify the initial hits. The screen setup should have distinction criteria to identify the initial hits. For example, when screening for antimicrobial activity, one should set a threshold for what is considered to be antimicrobial. If a high threshold is set, one would expect to have fewer hits overall. However, there is the risk of not finding any hits. While setting a low threshold one would expect more hits. Too many hits may be problematic to narrow down, especially if the proceeding assays are not high-throughput^{67,68}.

Minimum inhibitory concentration (MIC) assays, are a useful and standardized way to identify the minimum concentration needed for an antimicrobial to inhibit the growth of a microorganism after 17-24 hours. MICs can be run in high throughput using 96-well plates and small volumes (100 μ L). Growth is usually measured visually by observing bacterial pellet size, but one can also measure quantitatively through optical density (OD)⁶⁹. Potent antimicrobials will have a low MIC value, while antibiotics which are ineffective against a certain type of bacteria, for which resistance has emerged, will have a high MIC value⁷⁰.

After initial hits are identified and selected from the primary screen, further assays are run to narrow down the candidates. For example, checkerboard assays can be used to measure the interaction between two compounds against microbes^{71,72}. This test allows for the comparison of potency between the drug combination and the individual activities. Synergistic antibiotic-adjuvant combinations are ideal in a clinical setting since less antibiotic is needed to eradicate the bacteria which helps with prolonging resistance from occurring⁷³. Similar to MICs, checkerboard assays can be done in high-throughput and in small volume. However, in this case, there are two concentration gradients spanning from left to right across the x-axis and top to bottom on the y-axis. There are three types of interactions that can be seen between a drug combination: synergistic, antagonistic, and additive. A synergistic interaction occurs when the combined effect of the drugs is greater than the individual effects combined. Additive interactions are seen when the effect of the drug combination is equivalent to the individual effects. Finally, antagonism is seen when the effect of one drug lessens the effect of the other drug, resulting in a lower overall effect⁷⁴.

There are multiple methods to calculate the interaction of a drug combination, including the fractional inhibitory concentration (FIC) index, fractional maximal effect (FME), 3-D model approach, etc.⁷⁵. FIC index quantifies drug interactions by taking into account the MIC of the drugs when in combination and when used alone. This method has been used widely in the drug interactions literature^{76,77}. Testing several replicates and measuring the FIC at the 24-hour incubation mark, as opposed to longer incubations, will increase the likelihood of obtaining reputable and accurate results⁷⁵. The FME method quantifies the type of drug interaction while taking into account the effect of changing concentration ratios of the drugs on the degrees of interactions. This is ideal, as many drug interactions exhibit nonlinear pharmacodynamics. In this method, mathematical linearization is applied to the checkerboard results, and an isobologram-type data plot is produced⁷⁸. Prichard *et al.* described a 3-D approach to quantifying drug interactions. This involved elucidating the shape of the dose-response surface, identifying the regions of statistically significant synergy and antagonism, and quantifying the effects⁷⁹.

Exploring adjuvant mechanism of action

Mechanistic studies can be used to understand how an adjuvant is functioning in combination with an antibiotic. As mentioned above, adjuvants can function in many ways so the search space can be very broad. One can analyze the adjuvant's chemical structure, interaction profile, background (literature) to help narrow down the search for mechanism. For

example, if a chemical structure contains a beta-lactam ring, it is likely functioning as a beta lactam or targeting PBPs⁸⁰.

Adjuvants can synergize with antibiotics by targeting and interacting with the bacterial membrane. For example, AR-12, is an adjuvant that potentiates the activity of polymyxins against bacterial strains with acquired polymyxin resistance⁸¹. Polymyxins function by binding to the negatively charged phosphate group of the bacterial membrane, resulting in membrane disruption, and leads to cell death. Polymyxins pair well with bacterial membrane permeabilizers since they both target the bacterial membrane.⁸¹ Polymyxin resistance has emerged over the years and is becoming more apparent in the clinic.⁸² Bacteria are able to gain resistance to polymyxin through chromosomal mutations modifying the LPS.⁸³ The decline of anionic charge on the bacterial membrane results in less electrostatic binding of polymyxin.⁸⁴ It was found that AR-12 functions as a membrane permeabilizer. AR-12's function and adjuvant-like activity were shown from the results of the growth inhibition studies, time-kill assays and permeability assays using fluorescently labeled polymyxins. AR-12 potentially modifies the lipopolysaccharides, which alters the bacterial outer membrane, and thereby improves the uptake of polymyxin⁸¹.

One way to investigate if a compound is interacting with the bacterial membrane is through the use of fluorescent dyes like 3,3'-Dipropylthiadicarbocyanine Iodide (DiSC₃(5)) and 2',7'-Bis-(2-Carboxyethyl)-5-(and-6)-Carboxyfluorescein, Acetoxymethyl Ester (BCECF-AM)^{85, 86, 87}. DiSC₃(5) is a fluorogenic probe which can be used to measure changes in

transmembrane potential or configuration induced by membrane-altering compounds⁸⁶.

DiSC₃(5) accumulates on bacterial membranes and is translocated into the lipid bilayer, resulting in quenching of the fluorescence in the cell suspension. When the bacterial membrane is disrupted by an antibiotic or adjuvant, DiSC₃(5) is released from the lipid bilayer into the medium resulting in dequenching of fluorescence which can be measured in real-time⁸⁸.

BCECF, AM is a ratiometric pH indicator ideal for measuring changes in the cytosolic pH of cells. Unlike Disc3(5) which is adsorbed on the membrane, BCECF, AM enters the bacterial cell and is found in the cytoplasm⁸⁹. BCECF, AM increases in fluorescence in basic environments. By manipulating the pH of potassium phosphate (KP) buffer, the fluorescent signal either rises or falls when the membrane is breached⁹⁰. When the pH of the solution is higher than that of the bacterial cytoplasm (≈ 7.4), the intracellular pH increases after the membrane is breached, resulting in increased fluorescence⁹⁰. Glucose is used as a control in this assay to ensure that the system is functioning correctly. Glucose helps fuel the electron transport chain which then pumps protons outside of the cell. As a result of protons being pumped out of the cytoplasm, the pH will increase causing fluorescence to increase⁹¹.

Valinomycin is commonly used as a control to ensure that the BCECF, AM assay is functioning correctly. Valinomycin is a potassium-specific transporter, so it will transport potassium found in the buffer solution⁹². As a result of the potassium gradient, the potassium will then naturally exit the cell accompanied by a proton because it needs a charged ion in order to exit the cell. This will increase the cytosolic pH, resulting in an increase in fluorescence.

Repurposing drug-like compounds for antimicrobial use

One way to combat antimicrobial resistance is by identifying antimicrobial compounds and bringing them to the clinic at a faster rate. Repurposing well-characterized and approved drug-like compounds for antimicrobial purposes can speed up the discovery and development process since many of the characterizations have been completed⁹³.

The Pathogen Box was constructed to catalyze research on neglected disease drug discovery. It makes a suitable library source to identify potential antibiotic compounds against Gram-negative bacteria (Figure 2) since it contains drug-like compounds which have been well-characterized and developed⁹⁴. The Pathogen Box was constructed with compounds that show activity against tuberculosis, malaria, and kinetoplastids⁹⁵.

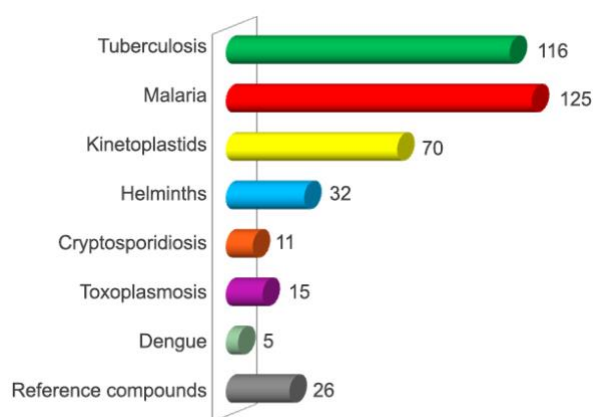


Figure 2: Distribution of therapeutic indications of the pathogen box compounds⁹⁵.

A study by Richter et al. found that compounds with primary amines on their structure can enter and accumulate into Gram-negative bacteria better⁹⁶. Primary amines can help compounds traverse through porins, which are hydrophilic channel proteins that play an important role in the metabolism of bacteria by allowing the uptake of nutrients and maintaining the electrochemical gradient across the outer membrane, contributing to the function of the proton motive force (PMF)^{96,97}. It does this through electrostatically interacting with the selective carboxylic acid found at the narrowest part of the porin, allowing entry of the compound⁹⁸.

Compound permeability can also be enhanced by EDTA, a metal chelator that has been used in the clinic since the 1950s to reduce and treat metastatic calcium deposits, angina, atherosclerotic, cardiovascular diseases, and more recently antimicrobial-related infections^{99,100,101,102}. EDTA destabilizes the bacterial LPS layer by sequestering divalent cations, especially magnesium and calcium¹⁰³. This creates permeable patches of phospholipid bilayer that lipophilic compounds, such as antibiotics, can pass through.¹⁰⁴ EDTA has been found to potentiate the activity of various antibiotics against resistant bacteria. At concentrations of ≈ 10 mM, EDTA functions in an adjuvant-like manner, while at higher concentrations EDTA exhibits antimicrobial activity.¹⁰⁵ One study used their newly discovered antimicrobial peptide, AA230, in combination with EDTA to function against MDR bacteria. EDTA decreased the effective AA230 dose by 2-4-fold.¹⁰⁶ AA230 is thought to also function through increasing the permeability of the bacterial membrane. EDTA can complement AA230's function by complementing the permeabilizing activity.¹⁰⁶

The Gram-negative bacteria, *Salmonella enterica* Typhimurium, causes about 1.35 million infections, 26,500 hospitalizations, and 420 deaths in the United States every year¹⁰⁷. During infection with *S. Typhimurium* the innate and adaptive immune systems are activated to eradicate the bacteria. Macrophage cells target the bacteria by engulfing it and releasing several substances (polypeptide hormones, complement components, coagulation factors, enzymes, etc.) to eliminate it¹⁰⁸. One compound that is greatly upregulated during this process is itaconate (ITA). As seen in figure 3, ITA functions by inhibiting isocitrate lyase at an inhibition constant of 120 μM . This enzyme is an essential part of the glyoxylate shunt, an anapleurotic pathway that bacteria use in carbohydrate-depleted environments, that catalyzes the production of succinate from isocitrate. Since the interior of macrophages are nutrient-poor environments, the *S. Typhimurium* must use the glyoxylate shunt for ATP and glucose production, and if the isocitrate lyase is inhibited, the cell will starve.

However, resistance emergence continues. *S. Typhimurium* is able to develop resistance against ITA by producing ITA-degrading enzymes such as: itaconate coenzyme A transferase (Ict), itaconyl-CoA hydratase (Ich), and (S)-citramalyl-CoA lyase (Ccl). These enzymes are also produced by other pathogens such as *Escherichia coli*. and *Mycobacterium* species^{109,110}. This allows the *S. Typhimurium* to persist and overcome the mechanism of the macrophage, leading to long-term infection.

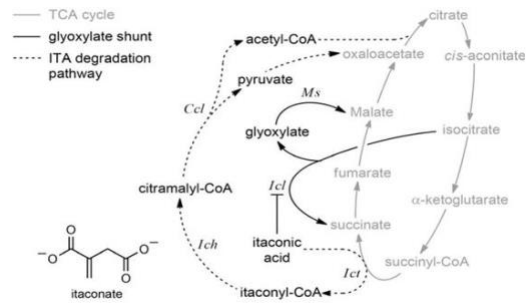


Figure 3: Schematic showing the tricarboxylic acid (TCA) cycle (grey), glyoxylate shunt (black), and ITA degradation pathway (dotted).

Hammerer *et al.* identified a compound, 3-nitro-pantothenate (3NP), that restored ITA function against resistant *Salmonella* Typhimurium¹¹¹. Their approach, coined bacterio-modulation, served to modulate bacterial metabolism to re-enable the host immune response. 3NP is thought to inhibit the ITA-degrading enzymes produced by the resistant bacteria, ultimately restoring macrophage function against *S. Typhimurium*. In combination, 3NP was able to decrease the MIC of ITA against *S. Typhimurium* to a similar sensitivity as *E. coli*, which is susceptible to ITA function¹¹¹. This reduction in ITA MIC is important since the cellular concentration in activated macrophages was found to be between 1 and 8 mM¹¹².

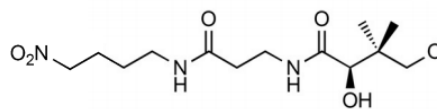


Figure 4: Structure of 3-nitro-pantothenate (3NP).

3NP was reported to have little to no antimicrobial activity against *S. Typhimurium*; it is only effective in combination with ITA. This characteristic may delay resistance from occurring

against 3NP if there is no genetic selection against it. This phenomenon was observed with co-amoxiclav, a combination of the antibiotic amoxicillin, and adjuvant clavulanate. It was found that by fine-tuning the adjuvant to antibiotic ratio, with higher adjuvant concentrations, the evolution of resistance can be steered and slowed⁴³.

In order to understand what mutations are occurring in bacteria and what effect they have on resistance, next-generation sequencing (NGS) could be used. This is a powerful technique that allows researchers to understand organisms at the genetic level. The cost to sequence genomes has drastically decreased over the last decade, allowing researchers to access this technology more readily¹¹³. There are several type of NGS technologies available such as Illumina HiSeq which is suitable for detecting SNPs in bacterial genomes¹¹⁴. Illumina provides high sequencing depth which increases sensitivity for SNP identification¹¹⁴. Illumina sequencers uses a method called sequencing by synthesis (SBS) which involves the detection of single bases as they are incorporated into growing DNA strands¹¹⁴. Illumina sequencing works by randomly breaking up the sample genomic DNA into fragments approximately 200-300 base pairs, attaching adapters to each end of the fragments, generating clusters through solid-phase PCR, and sequencing by synthesis using reversible terminators (figure 5)¹¹⁵.

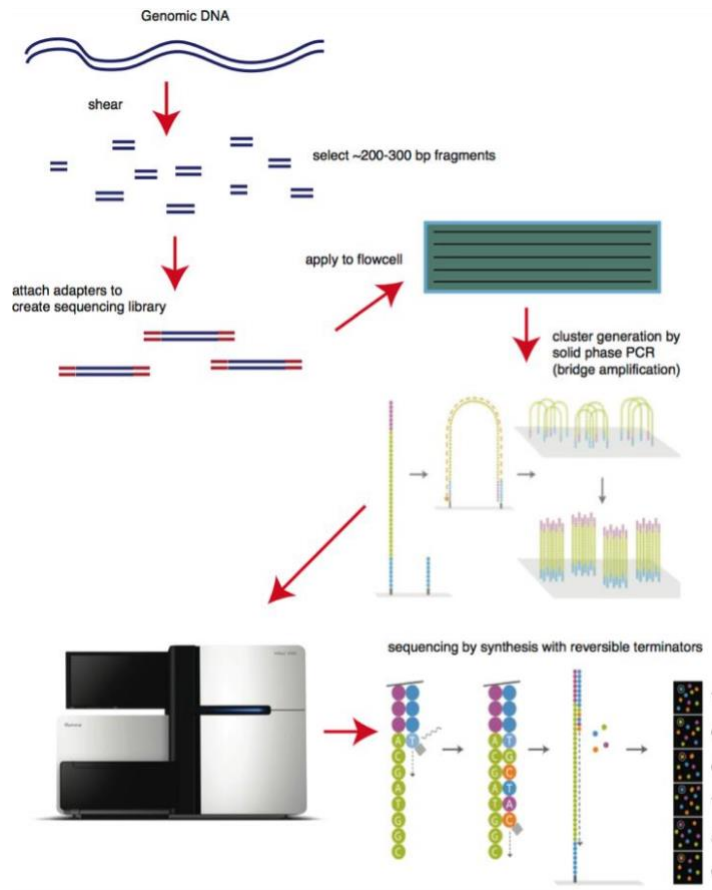


Figure 5: Illumina sequencing workflow¹¹⁶.

SNPs can be analyzed from bacterial clonal samples, where one genotype is present, and population samples, where many genotypes are present in a sample. To analyze the large amounts of sequencing data that is produced from NGS, a bioinformatics approach can be used. There are several tools and algorithms available to perform genomic analysis. SPAdes is an algorithm which helps with *de novo* genome assembly for single-cell and multi-cell bacterial data¹¹⁷. It works by first assembling graph constructions that detects and removes chimeric reads, aggregates the data into distance histograms, and tracks graph operations. The next step involves k-bimer adjustment which predicts accurate distance estimates between k-mers in the genome. Lastly, the paired assembly graphs and contigs are constructed.¹¹⁷

QUAST is a tool used for quality assessment of assembled genomes which can be done with or without a reference genome¹¹⁸. QUAST evaluates the following metrics: contig sizes, missassemblies and structural variations, genome variations and its functional elements, and variations of the N50 which assess contiguity of an assembly.¹¹⁸

Once a proper genome is assembled and validated, Snippy is used for variant calling to identify SNPs between the reference genome and the sequenced reads¹¹⁹. Snippy uses a tool to first align the reads to the reference genome and then identifies (calls) any variants. The calling process will also remove any artifacts¹¹⁹. Lastly, Snippy checks what effect these differences have on the sequenced reads and provides a readout detailing the mutations¹¹⁹.

The first objective of this thesis was to identify adjuvant compounds that are able to synergize with antibiotics and re-sensitize resistant bacteria. To do this, I performed a high-throughput screen using a small panel of structurally-diverse natural products and a number of antibiotic-resistant bacteria that had been generated in-house. One compound from this screen that was able to restore killing against one of the resistant strains was selected for further study, revealing that it allowed the passage of protons across the inner membrane of *E. coli*. The discovery of an adjuvant that is preferentially effective against resistant cells suggests that adjuvants may be able to combat the rise of antibiotic-resistant bacteria.

The second objective of this thesis was to repurpose drug-like compounds for antimicrobial use against Gram-negative. To do this, I screened compounds from the Pathogen Box to identify compounds that could kill Gram-negative bacteria in the presence of EDTA. Four lead compounds were selected for analog generation studies.

The third objective for this thesis was to understand resistance emergence against bacterio-modulation. To do this we generated and sequenced 3NP and ITA-exposed *S. Typhimurium* clonal and population sample. From the SNPs analysis, it was revealed that there was no genetic selection against 3NP. However, it was found that 3NP exhibited antimicrobial activity against *S. Typhimurium*.

Materials & Methods:

Chemicals and Plasticware:

All antibiotics used in this thesis were purchased from AK Scientific (Union City, USA). 3,3'-Dipropylthiadicarbocyanine Iodide (DiSC₃(5)) and 2',7'-Bis-(2-Carboxyethyl)-5-(and-6)-Carboxyfluorescein, Acetoxymethyl Ester (BCECF, AM) were purchased from Thermo Fisher Scientific (Waltham, USA). Cation-adjusted Muller-Hinton broth (CAMHB) was purchased from MilliporeSigma (Burlington, USA). Sterile 4-well nunclon treated culture dishes were also purchased from Thermo Scientific (cat. 167063). Falcon® clear round bottom untreated 96-well polystyrene microplates were used for MIC and checkerboards assays. Sterilin™ Standard 90mm Petri Dishes (Thermo Fisher, cat. 101R20) were purchased from Thermo Fisher Scientific (Waltham, USA). Pathogen Box library was provided by Medicines for Malaria Venture (MMV).

Natural product library:

Natural products were sourced from the InterBioScreen Natural Compound collection (Moscow, Russia), an assemblage of natural products weighted towards plant metabolites (60-65% of the whole). The ChemMine clustering tool was used to arrange the initial library of 68,000 natural products into a Newick hierarchical tree based on structural similarities and physicochemical properties.¹²⁰ Natural products were selected from nodes with at least two degrees of separation from the highest depth nodes in order to select diverse natural products. The molecular weight cut off was set to 600 Daltons (Da).

Strains

Table 1: Bacterial strains and suppliers used in the screen. SS indicating that the cells were selected for speed, i.e. the fastest swimmers.

Strains	Supplier
<i>Escherichia coli</i> MG1655 SS	Generated in-house ⁵⁹
<i>Staphylococcus aureus</i> ATCC 29213	American Type Culture Collection
<i>E. coli</i> clinical isolate 107115 (Canward).	CANWARD ICU Surveillance Studies ³⁸
<i>Escherichia coli</i> MG1655 PolyB ^r	Generated in-house ⁵⁹
<i>Escherichia coli</i> MG1655 azithromycin 2	Generated in-house ⁵⁹
<i>Escherichia coli</i> MG1655 doxycycline 2-3	This work
<i>Escherichia coli</i> MG1655 trimethoprim/sulfamethoxazole 2	Generated in-house ⁵⁹
<i>Escherichia coli</i> MG1655 cipro ^r	Generated in-house ⁵⁹
<i>Salmonella</i> Typhimurium	Auclair lab
<i>Salmonella Typhimurium</i> ITA ^r	This work (Nadia Sari (BSc Student, Findlay lab), Maxwell Miller(BSc Student, Findlay lab))

Escherichia coli MG1655 was a generous gift from Éric Déziel, INRS, Canada. *Staphylococcus aureus* ATCC 29213 was purchased from Cedarlane (Burlington, Canada). The *E. coli* clinical

isolate CANWARD 107115 was obtained from the Canadian Antimicrobial Resistance Alliance.^{38,39}

M9A+ media:

M9A is a nutrient-poor media which forces bacteria to grow using the glyoxylate shunt pathway. M9A+, formulated by Maxwell Miller (BSc student, Findlay lab), is a version of M9 media that includes several additives that allow the bacteria to grow easier in nutrient-poor conditions, while still requiring the glyoxylate shunt. M9A+ was used as the growth media for *S. Typhimurium* for 3NP evolutions studies.

Table 2: M9A+ ingredients.

M9A+ Ingredients:
M9 (1X Concentration)
0.4% Sodium Acetate
0.25% Agar
Histidine (40 mg/L)
Methionine (40 mg/L)
Proline (50 mg/L)
Arginine (150 mg/L)
Multi vitamin 0.01% (w/v) (Personelle "Senior" multivitamin, QC, Canada)
Distilled H ₂ O

Evolution of antibiotic resistance:

4-well Nunc-treated plates were raised on one side 8 mm, then molten 0.25% cation-adjusted Mueller-Hinton agar (CAMHA) was poured to half the height of the well on the lower side (0.45 cm). Once the agar had set (~20 min), the supports were removed and a second agar solution containing the antibiotic at a concentration 25X the naïve MIC of the respective antibiotic was added to an even depth. Plates were incubated overnight at room temperature to allow diffusion between the two layers. To initiate experiments, up to 75 µL of an overnight bacterial culture was inoculated in a line on the side of the well where the concentration of antibiotic was lowest. The wells were then covered with 3 mL of mineral oil to prevent desiccation and incubated at 37 °C for up to 10 days.

After cells had grown throughout the plate, agar was drawn from the far end of the plate (the area with the highest antibiotic concentration) into a p200 tip. This soft agar was then added to 5 mL of cation-adjusted Mueller-Hinton Broth (CAMHB), which contained the given antibiotic of interest at half its maximal concentration within the SAGE plate. Cells were incubated overnight at 37 °C, then either used directly in subsequent experiments or stored at -80 °C in 20% glycerol.

To initiate experiments, up to 75 µL of an overnight bacterial culture was inoculated onto the plate and evenly spread using a sterile spatula. The wells were then covered with up to 3 mL of mineral oil to prevent desiccation and incubated at 37 °C for 5 days.

After bacterial colonies had grown throughout the plate, mutants were harvested by sampling the end region of the plate (area with the highest antibiotic concentration and growth). The sample was then added to 5 mL of cation-adjusted Mueller-Hinton Broth (CAMHB) containing half the max concentration in the plate of the respective antibiotic and incubated overnight at 37 °C with shaking at 250 rpm. Cells were flash-frozen in liquid nitrogen and stored at -80 °C in 20% glycerol.

Generation of speed-selected E. coli strains

E. coli MG1655 cells were grown overnight in 5 mL of CAMHB at 37°C. Molten CAMHB was poured into a sterile 4-well nunclon-treated culture dish to the 50% height mark. Up to 75 µL of the overnight bacterial culture was inoculated in a line on one end of the plate. The wells were then covered with 3 mL of mineral oil and incubated at 37 °C. After growth across the plate, the cells that reached the end first were collected and inoculated into 5 mL of fresh CAMHB and grown overnight. These cells were then inoculated into a new sterile 4-well nunclon-treated culture dish and the process was repeated. This was done for a total of 4 times in order to select for the fastest swimmers. The overnight from the fourth sterile 4-well nunclon-treated culture dish was flash-frozen in liquid nitrogen and stored at -80 °C in 20% glycerol.

Generation of clonal and population samples

S. Typhimurium cells were challenged in SAGE plates with various concentrations of 3NP and or ITA (table 2). 3-NP was supplied by Dustin Duncan (PhD student, Auclair lab). Once the bacterial cells grew to the most concentrated side of the plate, 50 µl of solutions/agar was collected 2-3mm away from the edge of the plate and grown in 5 mL MHB which constituted the population samples. To create the clonal samples, the solution was then streaked onto MHA plates and grown for 24 hours. Colonies were picked and grown overnight in 5 mL of the respective media at 37°C. After growth, cells were flash-frozen in liquid nitrogen and stored at -80 °C in 20% glycerol . Clonal and population samples were generated by Nadia Sari (BSc student, Findlay lab) and Maxwell Miller (BSc student, Findlay lab). Table 3 shows a list of the population and clonal samples that were sent for genomic sequencing.

Illumina shotgun sequencing:

Illumina shotgun sequencing was completed by Nadia Sari (BSc student, Findlay lab). Genomic extraction of the population and clonal samples was conducted using the BioBasic EZ-10 Spin Column Genomic DNA Kit (Bacterial Samples). The DNA extracted from both the population and clonal strains was sent to Génome Québec's Nanuq for sequencing using HiSeq Illumina technology. The quality of the assembly output was then checked using FastQC (Galaxy Version 0.72) on the open-source platform Galaxy. The forward and reverse reads of each strain were assembled de novo using SPAdes 3.10.0 on Compute Canada's Cedar cluster. The resulting

assemblies were compared using Quast 5.0.2, and the reference genome for *Salmonella enterica Typhimurium* 14028 was obtained from the NCBI database.

Table 3: Samples sent for Illumina shotgun sequencing. Samples were either population-derived or clonal-derived.

	Population samples	Clonal samples
Conditions	<ul style="list-style-type: none"> • Sloped 7 mM 3-NP and constant 6.5 mM ITA in M9A+ • Sloped 7 mM 3-NP in M9A+ (3x) • Constant 6.5 mM ITA in M9A+ • Sloped 6.5 mM ITA in M9A+ • Sloped 7 mM 3-NP and constant 6.5 mM ITA in MHA • Sloped 7 mM 3-NP in MHA • Constant 6.5 mM ITA in MHA 	<ul style="list-style-type: none"> • <i>Salmonella enterica</i> Typhimurium ATCC 14028 - Obtained from Auclair Lab at McGill (OG) • Speed Selected Strain (SS) • Sloped 7 mM 3-NP and constant 6.5 mM ITA in M9A+ • Sloped 7 mM 3-NP in M9A+ • Sloped 6.5 mM ITA in M9A+ (3x) • Constant 6.5 mM ITA in MHA

Antibiotic Susceptibility Testing

The minimum inhibitory concentration (MIC) of all antibiotics was determined by broth microdilution according to Clinical and Laboratory Standards Institute guidelines.⁶⁹ Briefly, cells were grown overnight in 5 mL CAMHB at 37 °C with shaking at 250 rpm. Cells were then diluted into fresh media to the turbidity of a freshly prepared 0.5 McFarland standard. Cells were further diluted 1:100 in the same media, then mixed 1:1 with media containing the compound of interest in a 96-well plate polystyrene. Growth was evaluated by the naked eye after 16-20 hours of incubation at 37°C. Growth was ranked based on pellet size as full growth (>2mm

pellet), partial growth (~1mm pellet), minimal growth (<1 mm pellet), and no growth (no pellet).

High-throughput screen for adjuvants

An overnight culture *E. coli* was grown and diluted in MHB as described above for antibiotic susceptibility testing. Cells were then mixed 1:1 with each natural product at a final concentration of 12.5 mg/L. Where indicated the given antibiotic of interest was also added, at half its inhibitory concentration (a concentration where the cells would still grow in the absence of effective adjuvant). Controls were set in wells H10, H11, and H12 containing bacteria alone (growth control), the antibiotic alone at half its MIC positive control), or CAMHB without bacteria (sterility control). Plates were incubated at 37°C for 16-20 hr, then evaluated as described above for antibiotic susceptibility testing. A natural product was classified as a hit if it caused no inhibition of growth in the absence of antibiotic, but showed no growth, minimal growth, or partial growth in combination with a given antibiotic.

High-throughput screen of Pathogen Box compounds

The Pathogen Box compounds are supplied in five 96-well plates, containing 10 µL of a 10 mM dimethyl sulfoxide (DMSO) solution of each compound. Each compound was tested in the presence of EDTA or alone against *E. coli* MG1655 cells.

The pathogen box was screened in a 96-well plate format. Each well contained 1 μL of a unique pathogen box compound, 49 μL of LB media, 50 μL of 1:100 diluted McFarland Standard *E. coli* MG1655 cells with or without 5 mM EDTA for a total of 100 μL . For tests with EDTA, overnight bacterial culture was washed twice with, and resuspended in, MHB supplemented with 5 mM EDTA. Plates were incubated in a 37°C incubator for 20-24 hours. Plates were recorded for bacterial growth visually according to the following standard: Growth (>2 mm bacterial pellet), Partial growth (<2 mm bacterial pellet), and red wells indicated no visible growth (no bacterial pellet).

Pathogen box quality control

High resolution liquid chromatography-mass spectrometry was performed by Marcos Di Falco (Mass Spectrometrists, Concordia University). A 10 μL aliquot was analyzed by high resolution liquid chromatography-mass spectrometry using an Agilent 1260 Infinity II HPLC system (Agilent technologies, Santa Clara, CA, USA) connected in-line to 7 Tesla Thermo-Finnigan LTQ-FT mass spectrometer (Thermo Electron Corporation, San Jose, CA).

Chromatography separation of sample components was done using an Acquity BEH C18 2.1 x 50 mm, 1.7 μm column (Waters, Milford, MA). The solvents used to generate the gradient during reversed-phase separation were 0.1 % formic acid in water for Solvent A and 0.1% formic acid in acetonitrile for Solvent B. Solvent flow rate was 400 $\mu\text{L}/\text{min}$ and the gradient started at 10% B, increased in a linear gradient up to 90% B in 3 min, was kept at 90% B for 1 min, decreased to 2% B in 0.1 min and held at 10% B for 1 min. Column eluate was connected

to a Thermo-Finnigan Ion Max electrospray source. Spectra were acquired in positive mode from 250 to 1500 m/z at 50000 resolution at 400 m/z.

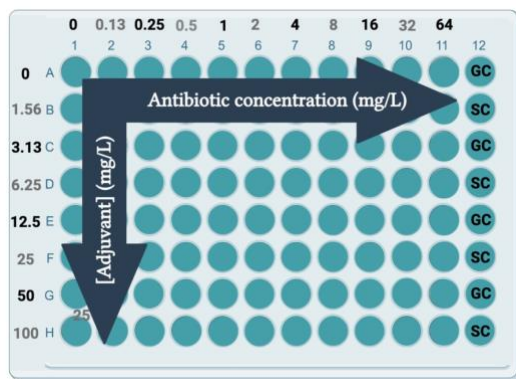


Figure 6: Checkerboard layout. Antibiotic concentration increases from left side of the plate to the right side. Concentrations doubling from each column to the next. Adjuvant concentration increases from top of the plate to the bottom. Concentrations doubling from each row to the next. Column 12 was used for control wells.

Checkerboard assays

Bacterial cells were prepared as described above for antibiotic susceptibility testing. 96-well plates were prepared with the antibiotics and their potential adjuvants in increasing concentrations as shown above in figure 6. Antibiotic concentrations increased along the x-axis, from 0 to 8x the MIC, while the adjuvant concentration increased along the y-axis from 0 to 100 mg/L. Fractional inhibitory concentration (FIC) indices were calculated according to equation 1:

$$FIC = \left(\frac{C_A}{MIC_A} \right) + \left(\frac{C_B}{MIC_B} \right)$$

Where MIC_A and MIC_B are the minimum inhibitory concentrations of compound A and B, respectively. C_A and C_B are the concentrations of the drugs in combination. A value that is less

than 0.5 indicates synergism, from 0.5–1 indicates additive effects, from 1-2 indifference, and greater than 2 antagonism.

Membrane depolarization assay

Naïve and resistant bacteria were inoculated from -80 °C stocks into 5 mL CAMHB and incubated overnight at 37 °C with shaking at 225 rpm. Cells were centrifuged at 1300 rpm for 3 minutes. Supernatant was removed and resuspended in 5 mM sodium HEPES buffer, pH 7.4, containing 20 mM glucose. This process was repeated for a total of 3 times, after which they were resuspended in 5 mM sodium HEPES buffer, pH 7.4, containing 20 mM glucose plus 0.1M KCl at an OD of 0.05. The cells were then incubated with 1.2 M DiSC₃(5) for 10 minutes in a 3 mL quartz fluorescence cuvette, then placed in a Cary Eclipse fluorescence spectrometer. Fluorescence measurements were taken at excitation 670 nm and emission 622 nm, with a slit width of 10 nm. 1% Triton-X was used as a positive control.

Internal bacterial pH was measured with BCECF, AM.¹⁸ Naïve *E. coli* MG1655 cells were inoculated from -80 °C stocks into CAMHB at 37 °C, with shaking at 225 rpm. 5 mL overnight solutions was spun at 13.3 Kg⁻¹ for 1 minute, the supernatant was discarded, then the cells were resuspended in 1.5 mL of 50 mM potassium phosphate buffer, pH 8. This process was repeated a total of 3 times, then the cells were suspended in 60 µl of potassium phosphate buffer, pH 8, and stored at room temperature. 5 µL of prepared cells was added to 1 mL of the 5 mM EDTA in the same buffer, alongside 20 µL of 1 mM BCECF, AM. The mixture was then added to a 3 mL quartz fluorimeter cuvette and placed in the fluorimeter. Fluorescence was measured at an

excitation wavelength of 504 nm and emission wavelength of 527 nm using the kinetics program on Cary Eclipse fluorescence spectrometer with measurements set every second. After 1 minute of measurements 1 μ L of 1 M glucose was added. Once the fluorescence intensity stabilized, 1 μ L of 25 mg/ml valinomycin was then added, followed by either 10 μ L of 10 mg/ml Perforone or 64 μ L of 1 mg/mL polymyxin B. The solution was thoroughly mixed by pipette immediately after each compound was added.

RESULTS:

The primary screen

As seen in figure 7, I began by creating a small, diverse natural product library. The 68,000 compounds in the InterBioScreen Natural Compound Collection were passed through ChemMine, sorting them into a hierarchical tree based on chemical similarity. From this tree 99 compounds with molecular masses of 600 Da or less were then purchased, keeping at least two nodes of separation between each compound. 74 of these were soluble in DMSO to a concentration of 25 mg/L, and were used in the screen.



Figure 7: Adjuvant discovery pipeline

Table 4: MICs of naïve and resistant MG1655 *E. coli* cells.

Antibiotics	Naïve MG1655 (mg/L)	Resistant cells MIC (mg/L)
Polymyxin	4	256
Ciprofloxacin	0.015	8
Trimethoprim/ Sulfamethoxazole	0.0625 / 1.1875	16 / 304
Azithromycin	4	128
Doxycycline	0.25	60

E. coli MG1655 mutants which were independently resistant to azithromycin, ciprofloxacin, doxycycline, polymyxin B, and the combination of sulfamethoxazole and trimethoprim were drawn from prior experiments,⁵⁹ or were generated by passage of naïve cells through SAGE plates containing the respective antibiotic at a minimum of 10x the initial MIC (Table 4). Both naïve and resistant cells were then screened for susceptibility to each compound in the natural product library at 50 mg/L, either alone or in the presence of each antibiotic/antibiotic pair at half their MIC. The results of these 17 screens are summarized in Figure 8.

i



ii

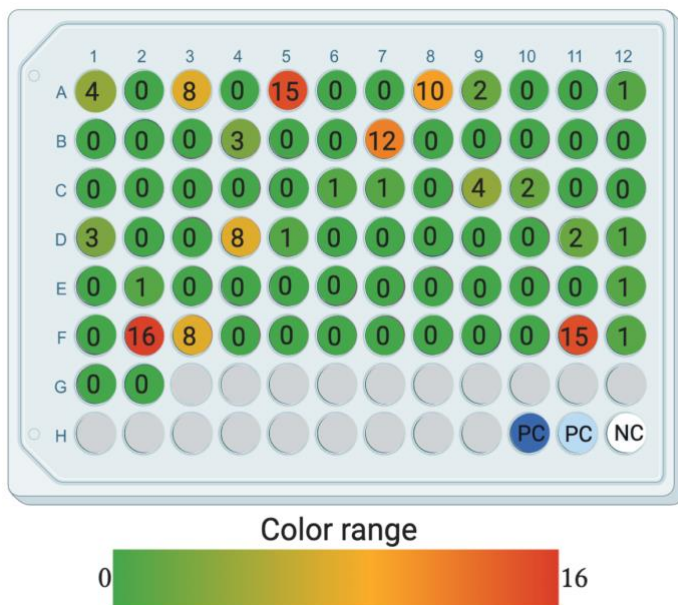


Figure 8: Primary screen results i) Growth inhibition assay of each individual plate from the primary screen. Green wells indicate growth (>2 mm bacterial pellet), yellow wells indicate partial growth (<2 mm bacterial pellet), and red wells indicate no visible growth. Compound positions are conserved across the screens. ii) Data from i, condensed into a single plate. Values indicate the number of plates where the natural products well had no growth.

Five of the compounds inhibited bacterial growth in half or more of the conditions. This includes **1** (well A05, Figure 8), a derivative of the histological dye hematoxylin known as hematein¹²¹. Hematein is a known casein kinase II inhibitor able to inhibit cancer growth,¹²² and while its activity against bacteria has not been previously reported, the closely related analogue brasilin is a known inhibitor of Gram-positive (but not Gram-negative) bacteria.¹²³ Other notable antimicrobial compounds include **2** (well B07, Figure 8), an analogue of the well-characterized adjuvant rutin.^{124,125} While generally lacking in direct antimicrobial activity, rutin enhances the killing effect of other flavones. Against *E. coli* rutin has been reported to interfere with biofilm formation and virulence factor production, by reducing the secretion of quorum sensors.¹²⁶ Well F02 contained the well-known antibiotic doxycycline as a positive control, which as expected inhibited the growth of every bacteria but the doxycycline-resistant strain.

Sixteen of the compounds in the screen synergized with one or more of the antibiotics tested, and six of these were specific for antibiotic-resistant strains. This included **3** (ononin, well A01), the compound ononin, which inhibited the growth of resistant bacteria when combined with azithromycin, ciprofloxacin, or the sulfamethoxazole/trimethoprim combination, and weakly inhibited doxycycline-resistant cells when combined with doxycycline. Ononin has very weak antimicrobial activity, but like many flavones can rigidify the bacterial membrane at high concentrations.¹²⁷ Also of interest was **4** (ugaferin, well C09), which inhibited bacterial growth when combined with doxycycline and weakly inhibited growth with ciprofloxacin, polymyxin B, and the sulfamethoxazole/trimethoprim combination. Originally

isolated from the roots of the plant, *Ferula ugamica*, ugaferin had no previously reported bioactivity.¹²⁸

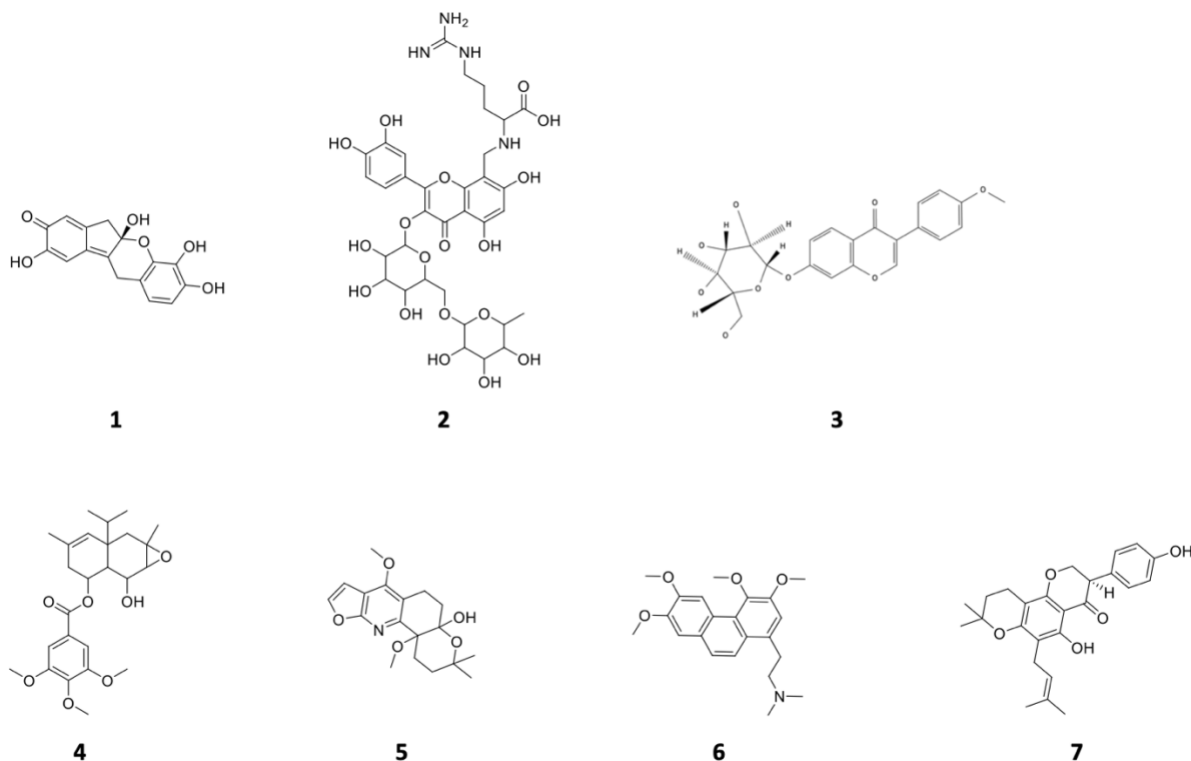


Figure 8: Hit candidates from the primary screen. 1: hematoxylin, 2: rutin 3 ononin, 4: ugaferin, 5: perforone, 6: N,N-dimethyl-2-(3,4,5-trimethoxyphenyl)ethanamine, 7: (3R)-5-hydroxy-3-(4-hydroxyphenyl)-8,8-dimethyl-6-(3-methylbut-2-enyl)-2,3-dihydropyrano[2,3-h]chromen-4-one.

Six adjuvant candidates were brought forward from the primary screen for further evaluation. As seen in figure 10, the candidates had different activity profiles. For example, perforone, a single hit, was found to be effective against resistant bacteria in combination with polymyxin. B7, on the other hand was found to be antimicrobial or adjuvant-like, depending on the bacteria strain and antibiotic it was paired with. Checkerboard assays were used to evaluate the interaction between the six adjuvant candidates in combination with the panel of antibiotics. To quantify the degree of synergy, fractional inhibitory concentration index (FIC)

was employed¹²⁹. A combination of molecules is considered synergistic when the FIC ≤ 0.5 . Of all combinations, perforone, exhibited the lowest FIC (0.1-0.29) when paired with polymyxin. It was able to reduce the amount of polymyxin needed by ~ 16 -fold.

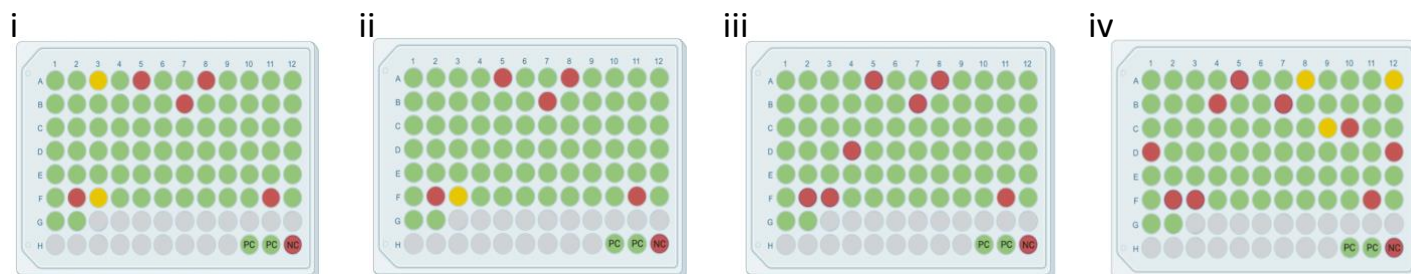


Figure 9: Validation screen of library of natural products using PMBN compared to polymyxin B. i) Polymyxin B 2 cells + PMBN (8 mg/L) + NP, ii) MG1655 cells + PMBN (0.1 mg/L) + NP, iii) Polymyxin B 2 cells + NP, iv) Polymyxin B 2 cells + poly B (8 mg/L) + NP. Green wells indicate growth (>2 mm bacterial pellet), yellow wells indicate partial growth (<2 mm bacterial pellet), and red wells indicate no visible growth (no bacterial pellet).

As polymyxin B is able to destabilize the outer membrane of *E. coli*, potentially allowing compounds entry into the cell¹³⁰, we were concerned that the inhibitory activity seen might be due to improved access of perforone to the interior of the cell rather than to an improvement in polymyxin B function. We thus repeated the initial screen with polymyxin B nonapeptide (PMBN), an analogue that is still able to permeabilize bacterial membranes, but lacks both the acyl tail and its antimicrobial activity.¹³¹ No inhibition was observed when perforone and PMBN were applied together (Figure 9), suggesting that the activity we observed against polymyxin B-resistant *E. coli* was due to resensitization of the bacteria to polymyxin B or to synergy between the two compounds.

Hits	Activity	ANTIBIOTICS																	
		Doxycycline			Azithromycin		Polymyxin B		Polymyxin B nonapeptide			Ciprofloxacin			Trimethoprim/Sulfamethoxazole			None	
		Resistant		Naive	Resistant		Resistant		Resistant		Naive		Resistant		Naive		Resistant		Naive
		NP	Ab+NP	Ab+NP	NP	Ab+NP	NP	Ab+NP	NP	Ab+NP	Ab+NP	NP	Ab+NP	Ab+NP	NP	Ab+NP	Ab+NP	NP	
A5	Antimicrobial	0	1	1	1	1	1	1	1	1	1	1	0	1	1	1	1	0.5	
A12	Adjuvant (single hit)	0	0	0	0	0	0	0.5	0	0	0	0	0	0	0	0	0	0	
B7	Adjuvant & antimicrobial	0	1	0	1	1	1	1	1	1	1	0	0.5	1	0	0.5	1	0	
C9	Adjuvant	0	1	0	0	0	0	0.5	0	0	0	0	0.5	0	0	0.5	0	0	
C10	Adjuvant	0	1	0	0	0	0	1	0	0	0	0	0	0	0	0	0	0	
F12	Adjuvant (single hit)	0	0.5	0	0	0	0	0	0	0	0	0	0	0	0	0	0	0	

Figure 10: Primary screen activity profile of the 6 selected candidates paired with the panel of antibiotics against bacterial cells (naïve and resistant). Exhibiting the activity and specificity of hit candidates that were effective with which antibiotic and which type of bacteria. Green cells with 1's indicated that this pairing was effective in killing the cells. Yellow cells with 0.5's indicated that this pairing partially inhibited bacterial growth. 0's indicated that the pairing did not inhibit bacterial growth.

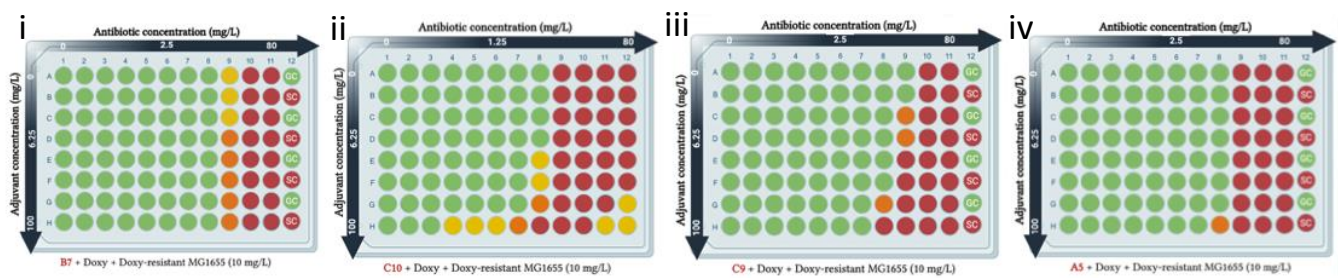


Figure 11: Synergy between doxycycline and adjuvant candidates against doxycycline-resistant *E. coli* cells checkerboard assays. i) B7 + doxycycline. ii) C10 + doxycycline. iii) C9 + doxycycline. iv) A5 + doxycycline. Checkerboard assays used to measure the interaction between adjuvant candidates and doxycycline. Green indicates growth (>2 mm bacterial pellet), yellow wells indicate partial growth (<2 mm bacterial pellet), and red wells indicate no visible growth.

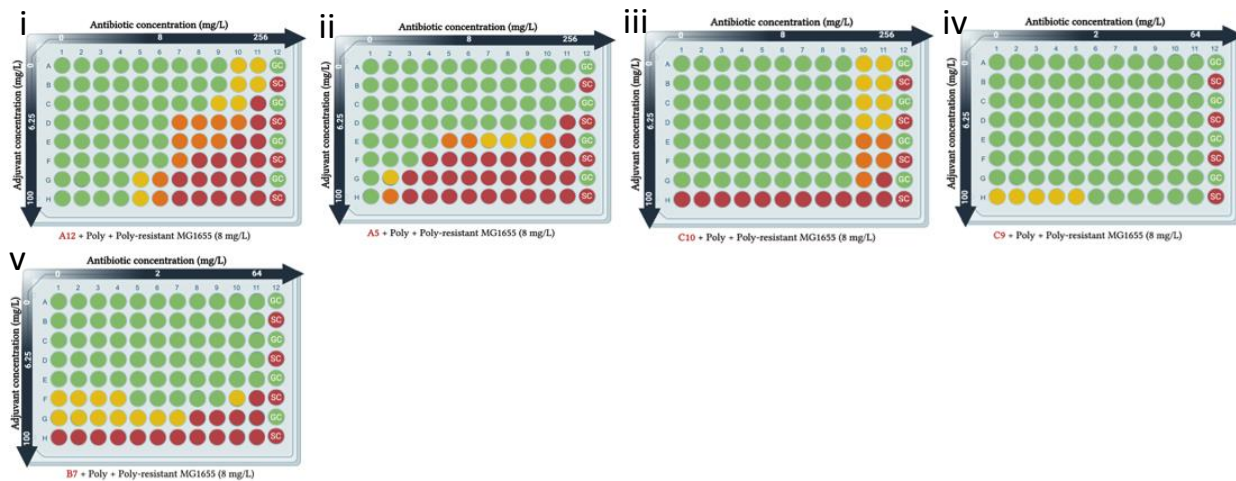


Figure 13: Synergy between polymyxin and adjuvant candidates against polymyxin-resistant *E. coli* cells. i) A12 + polymyxin + poly-resistant cells. ii) A5 + polymyxin + poly-resistant cells. iii) C10 + polymyxin + poly-resistant cells. iv) C9 + polymyxin + poly-resistant cells. v) B7 + polymyxin + poly-resistant cells. Checkerboard assays were used to measure the interaction between adjuvant candidates and azithromycin.

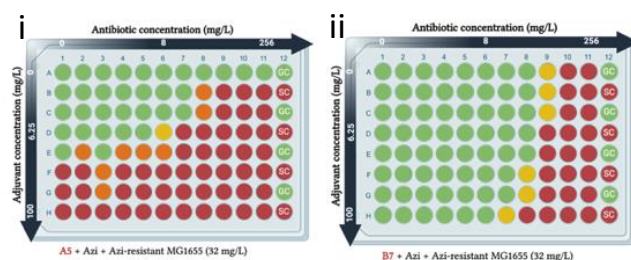


Figure 14: Synergy between azithromycin and adjuvant candidates against azithromycin-resistant *E. coli* cells. i) A5 + azithromycin. ii) B7 + azithromycin. Checkerboard assays used to measure the interaction between adjuvant candidates and azithromycin. Green indicates growth (>2 mm bacterial pellet), yellow wells indicate partial growth (<2 mm bacterial pellet), and red wells indicate no visible growth.

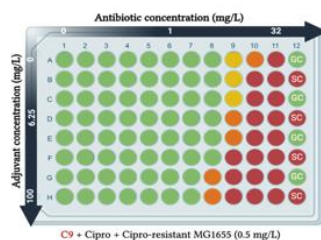


Figure 15: Synergy between ciprofloxacin and adjuvant candidates against ciprofloxacin-resistant *E. coli* cells. C9 + ciprofloxacin. Checkerboard assays used to measure the interaction between adjuvant candidates and ciprofloxacin. Green indicates growth (>2 mm bacterial pellet), yellow wells indicate partial growth (<2 mm bacterial pellet), and red wells indicate no visible growth.

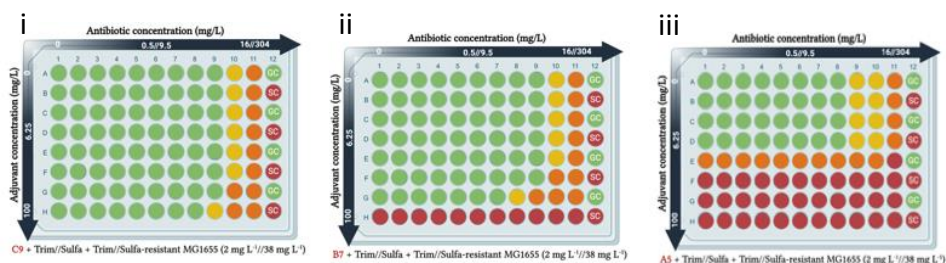


Figure 16: Figure 15: Synergy between trimethoprim/ sulfamethoxazole and adjuvant candidates against trimethoprim/sulfamethoxazole-resistant *E. coli* cells. i) C9 + trimethoprim/ sulfamethoxazole. ii) B7 + trimethoprim/ sulfamethoxazole. iii) A5 + trimethoprim/ sulfamethoxazole. ii) B7 + trimethoprim/ sulfamethoxazole. iii) A5 + trimethoprim/ sulfamethoxazole. Checkerboard assays used to measure the interaction between adjuvant candidates and trimethoprim/ sulfamethoxazole. Green indicates growth (>2 mm bacterial pellet), yellow wells indicate partial growth (<2 mm bacterial pellet), and red wells indicate no visible growth.

The checkerboard assays showed a range of activities depending on the candidate natural product and antibiotic combinations. A notable example is compound **1**, (A05,

hematoxylin), which synergized with four antibiotics as measured by checkerboard and FIC. However, this compound was found to be antimicrobial against the resistant bacteria (FIC of 0.3125 in combination with azithromycin). As mentioned above, compound **1** is hematein, a known compound with antimicrobial activity. Interested in compounds that could selectively restore activity against antibiotic-resistant bacteria, we focused on an analogue of perforone,¹³² compound **5** (well A5) (Figure 16). Referred hereafter as perforone, **5** is a hemiketal originating from the plant, *Haplophyllum perforatum* which is distributed throughout central Asia. *H. perforatum* produces more than 30 quinolinic alkaloid compounds, including perforone¹³². No relevant literature was found on perforone's, or any substructure's, activity as an adjuvant or antibiotic. Perforone weakly inhibited the growth of polymyxin B-resistant *E. coli* when combined with polymyxin B at half its MIC. A checkerboard assay confirmed synergy between the two compounds, with a minimal FIC of 0.19 and a 16-fold reduction in the MIC of polymyxin B (Figure 17). However, this synergy was only present against the polymyxin B-resistant *E. coli*. Perforone's effect was at best additive against *E. coli* MG1655, with a 2-fold reduction in polymyxin's MIC at 100 mg/L of perforone (Figure 17). This shows that perforone is more effective against resistant cells. A similarly small effect was observed with *S. aureus* ATCC 29213 and the antimicrobial peptide melittin. Addition of perforone to the mixture improved the activity of melittin 2-fold, at 75 mg/L of perforone (Figure 18).

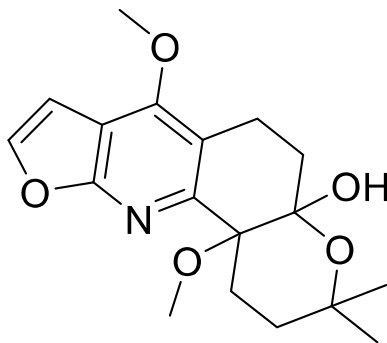


Figure 17: Structure of perforone.

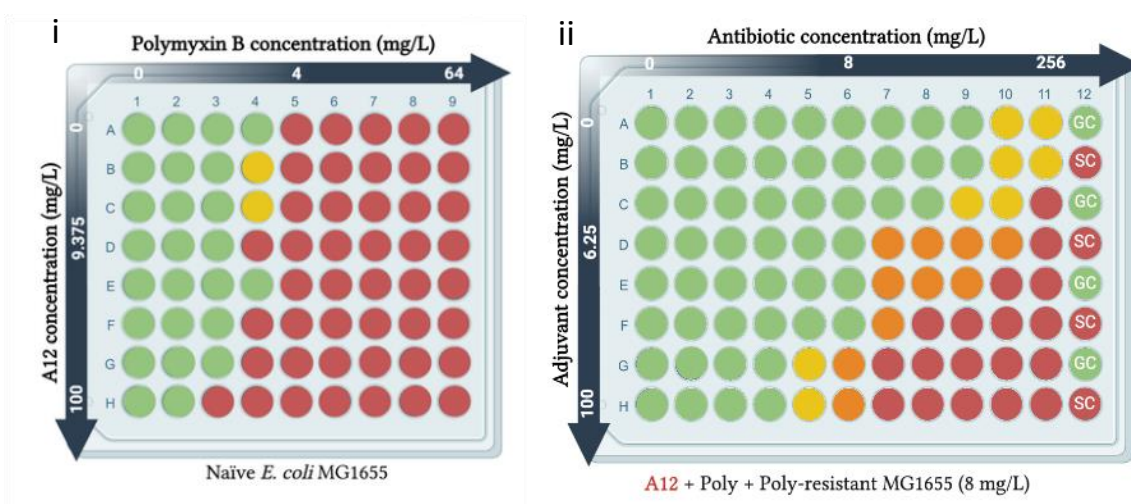


Figure 18: i) Synergy between perforone and polymyxin against naïve MG1655. ii) Synergy between perforone and polymyxin against polymyxin-resistant cells. Checkerboard assays used to measure the interaction between perforone and polymyxin. Green indicates growth (>2 mm bacterial pellet), yellow wells indicate partial growth (<2 mm bacterial pellet), and red wells indicate no visible growth. Perforone in combination with polymyxin against polymyxin-resistant cells exhibited an FIC of 0.19, indicating synergistic interaction. Perforone in combination with polymyxin against naïve MG1655 cells exhibited an FIC of 0.625, indicating an additive interaction.

In the primary screen, perforone was only synergistic with polymyxin, and not with other antibiotics. This led us to evaluate if perforone's activity was specific to membrane permeabilizing antibiotics. To test this we did a checkerboard assay using perforone and melittin, a honeybee venom-derived antimicrobial peptide that targets the bacterial membrane, against *S. aureus* ATCC 29213. This checkerboard also provided insight on if perforone is effective against Gram-positive bacteria like *S. aureus*. The FIC was found to be

0.75, indicating an additive interaction between perforone and melittin. Perforone was able to enhance the activity of melittin and reducing the amount of antibiotic needed by 4x. Although the interaction wasn't synergistic like in the combination of perforone and polymyxin, it still demonstrates that perforone functions with membrane-permeabilizing antibiotics. It can also be concluded that perforone is effective against Gram-positive bacteria, in addition to Gram-negative.

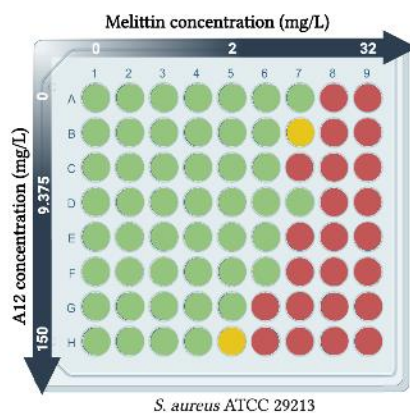


Figure 19: Synergy between perforone and melittin against *S. aureus* ATCC 29213. Checkerboard assay was used to measure the interaction between perforone and melittin. Green indicates Growth (>2 mm bacterial pellet), yellow wells indicate partial growth (<2 mm bacterial pellet), and red wells indicate no visible growth. Perforone in combination with melittin against *S. aureus* ATCC 29213 cells exhibited an FIC of 0.75, indicating an additive interaction.

Perforone allows protons to flow across the membrane

Prior sequencing of the poly-resistant *E. coli* strain revealed a number of mutations in genes responsible for lipopolysaccharide biosynthesis⁵⁹, suggesting that perforone might act via interactions with the outer bacterial membrane. We thus studied the effect of perforone on the proton motive force, using the fluorogenic probe DiSC₃(5).⁸⁶ DiSC₃(5) accumulates on the inner

bacterial membrane, suppressing its own fluorescence. When this membrane is permeabilized the dye diffuses into the cell, leading to a measurable increase in fluorescence.⁸⁶

In our hands addition of polymyxin B led to the expected increase in fluorescence (Figure 18).⁸⁸ Unfortunately, addition of perforone to DiSC₃(5) in the absence of cells lead to a rapid loss of fluorescence, indicating unintentional quenching of the dye. We thus increased the pH of the media to 8.0 and switched to 2',7'-bis(2-carboxyethyl)-5,6-carboxyfluorescein acetoxymethyl ester (BCECF, AM), a ratiometric pH indicator ideal for measuring changes in the cytosolic pH of cells. Unlike DiSC₃(5), which is adsorbed onto the membrane, BCECF, AM localizes to the cytoplasm.^{18,133} This was expected to prevent premature quenching of the dye, as permeabilization of the inner membrane will basify the cytoplasm (and increase fluorescence by BCECF, AM) before perforone is able to amass significant intracellular concentrations.

Under these conditions, addition of perforone increased fluorescence 8.5 to 29.2 arbitrary units, followed by a decrease back to 19.7 AU over a span of four minutes (Figure 8). Polymyxin B rapidly increased fluorescence and had no slow quenching effect, suggesting that while perforone is also able to quench BCECF, AM, both compounds are able to dissipate the bacterial proton motive force.

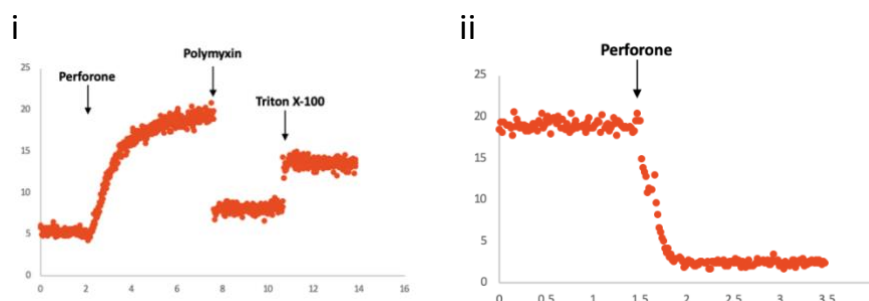


Figure 20: Measuring changes in transmembrane potential using DiSC₃(5). i) Fluorescence following the addition of perforone and polymyxin B to polymyxin-resistant *E. coli* cells (polyBr). 1% triton X-100 was used to fully quench the system. ii) Addition of perforone to DiSC₃(5) absent bacterial cells. Fluorescence was measured at an excitation $\lambda = 670$ nm and emission of $\lambda = 622$ nm, with measurements every second.

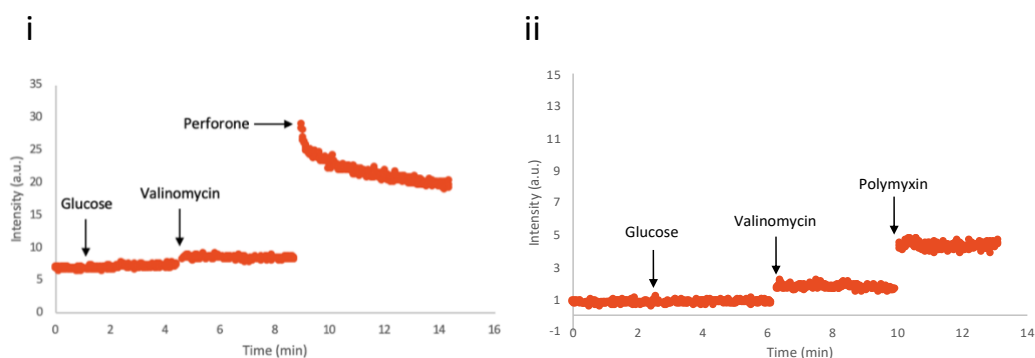


Figure 21: Measuring *E. coli* MG1655 cytosolic pH with BCECF, AM. A) Addition of Perforone. B) Addition of polymyxin B. Fluorescence was measured at an excitation $\lambda = 504$ nm and emission $\lambda = 527$ nm, with measurements every second.

Table 5: Summary of Pathogen Box screen.

Number of compounds	400
Number of compounds that require EDTA to show activity	33
Number of compounds that passed QC (RP-LCMS)	24
Number of selected compounds for amine addition	4

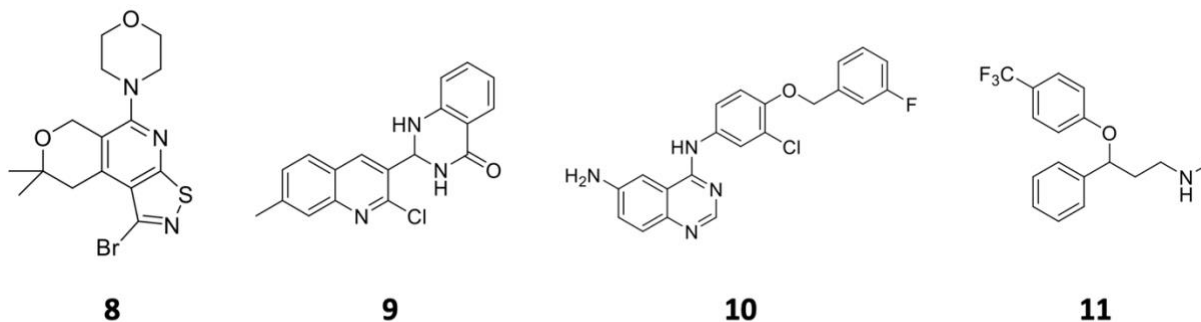


Figure 22: Pathogen Box lead candidates.

Pathogen Box Screen:

I began by screening the 400 Pathogen Box compounds against *E. coli* MG1655 cells for susceptibility to each compound in the library, either alone or in the presence of EDTA. I was specifically looking for compounds that could exhibit antimicrobial activity if it entered into the bacterial cell, i.e. compounds that inhibited growth in the presence of EDTA, but not alone. The results of the screen are summarized in table 5. 33 compounds required EDTA to exhibit antimicrobial activity against *E. coli* MG1655. Quality checks were then completed using RP-LCMS to ensure that the compounds were single compounds. 24 of the 33 compounds passed this test. Of these, 11 showed half inhibition, and 13 showed full inhibition. **9**, (4(1H)-Quinazolinone, 2-(2-chloro-7-methyl-3-quinolinyl)-2,3-dihydro), a derivative of a known antimicrobial, quinoline, exhibited half inhibition in combination with EDTA. **9** was found to possess antitumor properties as it inhibits the human 20S proteasome¹³⁴. While **10** exhibited full inhibition against *E. coli* MG1655 in combination with EDTA. **10** is also a derivative of quinoline, and was found to target epidermal growth factor receptor (EGFR) and carbonic anhydrase IX (CAIX) which contribute to non-small cell lung cancer¹³⁵. Quinolones function as an antimicrobial by targeting bacterial DNA gyrase (topoisomerase II) and topoisomerase IV,

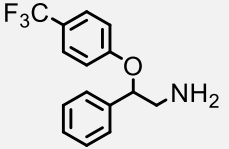
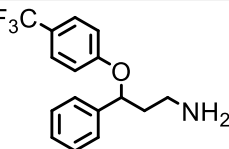
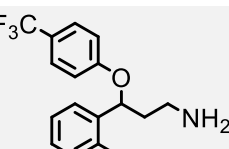
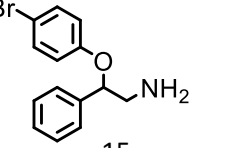
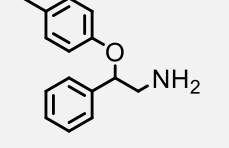
which leads to inhibition of DNA replication^{136,137}. Since **9** and **10** are derivatives of quinoline, they have the potential to be an effective Gram-negative antimicrobial after analog generation studies.

Compounds were selected for analog generation studies based on criteria outlined by Richter, *et al*⁹⁶, i.e., low number of rotatable bonds (flexibility), low globularity, molecular mass less than 500 Da, and suitable positions for primary amine addition. As seen in figure 22, the selected candidates possess less than three rotatable bonds, less than 400 Da, low globularity, and at least two positions for primary amine addition. For example, **8** (H-Isothiazolo[5,4-b]pyrano[4,3-d]pyridine, 1-bromo-8,9-dihydro-8,8-dimethyl-5-(4-morpholinyl)), a known anticonvulsant, exhibited full inhibition against *E. coli* MG1655 in combination with EDTA, has a molecular weight of 384.3 Da, 2 rotatable bonds, and 6 potential sites for primary amine addition.

Four lead compounds were then selected for further analogue generation through primary amine addition (figure 22) by Phil Prevost (MSc Candidate, Forgione lab). Preliminary antibiotic characterization studies on analogs of **11**, a derivative of a known SSRI with antidepressant activity, fluoxetine has commenced by Farhan Chowdhury (Msc Candidate, Findlay lab) . Fluoxetine has also been reported to have adjuvant-like activity with ciprofloxacin and fluconazole against *E. coli* and *Candida albicans*. It is hypothesized that fluoxetine may inhibit cell wall formation, cell division or cell membrane distraction¹³⁸. It is possible that our efforts toward analog generation may also help increase fluoxetine's activity as an adjuvant. Future studies will involve testing for both antibiotic activity and adjuvant-like activity. Five

analogs of **11** were tested via MIC assays against *Enterococcus faecium* 130816 UoM, *S. aureus* ATCC 29213 *Klebsiella pneumoniae* CANWARD 115252, *Acinetobacter baumannii* ATCC 19606, *Pseudomonas aeruginosa* CANWARD 114089, *E. coli* CANWARD 111953, and *E. coli* ATCC 25922. Most of the analogs have poor activity with a MIC greater than. Compound 12-16. **14** exhibited the best activity with an MIC of 32 µg/mL against *E. faecium* 130816 UoM and *S. aureus* ATCC 29213. However, it was ineffective against the Gram-negative strains exhibiting an MIC > 128 µg/mL. **12, 13, 15, 16** exhibited poor activity with MICs > 64 µg/mL. This indicates that these modifications of **11** did not contribute to an increased antimicrobial activity. More studies are underway to test **12-16** for adjuvant-like activity by Farhan Chowdhury (Msc Candidate, Findlay lab). Phil Prevost (MSc Candidate, Forgiione lab) is generating more analogs of **11**, as well as **8-10**.

Table 6: Activity of generated analogs of compound 11.

	MIC						
	Gram-Positive (µg/mL)		Gram-Negative (µg/mL)				
	<i>E. faecium</i> 130816 UoM	<i>S. aureus</i> ATCC 29213	<i>K. pneumoniae</i> CANWARD 115252	<i>A. baumannii</i> ATCC 19606	<i>P. aeruginosa</i> CANWARD 114089	<i>E. coli</i> CANWARD 111953	<i>E. coli</i> ATCC 25922
 12	256	256	256	256	>256	256	256
 13	64	64	128	64	256	128	64
 14	32	32	128	128	256	256	128
 15	64	128	256	128	>256	128	128
 16	128	128	>256	256	>256	>256	>256
AMPICILLIN	4	4	128	>256	>256	>256	8

Bacterio-modulation genomic analysis:

As described in the methods, population and clonal samples were prepared by Nadia Sari (BSc student, Findlay Lab) and Maxwell Miller (BSc student, Findlay Lab) and sent for

Illumina shotgun sequencing. The sequencing data from each sample was analyzed using bioinformatics approach involving *de novo* genome assembly via SPAdes, quality control via Quast, and SNP variant calling via Snippy to compare the genomes of the experimental samples to the reference genome and specifically identify the SNPs that differed. As seen in figure 21, there were 18 total SNPs found in the population samples. 11 of these were synonymous mutations, while, 7 SNPs were found to be nonsynonymous. The genes that were by these mutations had functions related to the inner membrane protein, flagella regulation, hydrolase, transcription regulator, ATPase, symporter, and enterochelin esterase activity. As mentioned, 3NP was proposed to function as an ITA-degrading enzyme inhibitor to resensitize *S. Typhimurium* to ITA¹¹¹. The SNPs found in the population samples do not directly or indirectly target 3NP function, indicating that there is no genetic selection against 3NP in the population samples.

Samples	Position	Allele	Effect	Gene name	Gene Function
3NP M9A	9854	A	missense	yaaH	Inner mem protein
3NP ITA M9A	1412907	C	missense	ynic	2-deoxyglucose-6-phosphatase activity
ITA M9A	1433140	T	stop gained	ydiv	Regualtion flagella
3NP ITA MHA	1530118	A	missense	slyA	Transcription regulator. Activates expression of genes such as molecular chaperones, the starvation lipoprotein (slp). Represses expression of genes involved in the histidine biosynthetic pathway
3NP M9A	1923738	C	missense	minD	ATPase required for the correct placement of the division site. Cell division inhibitors
ITA MHA	2093569	C	intergenic region	STMI4 2425-seru	Regulation adapters that allow synthesis of proteins from MRNAS
3NP MHA	2093576	A	intergenic region	STMI4 2425-seru	Regulation adapters that allow synthesis of proteins from MRNAS
3NP ITA M9A	2093590	A	non coding transcript exon	serU	Regulation adapters that allow synthesis of proteins from MRNAS
ITA M9A	2093597	C	non coding transcript exon	serU	Regulation adapters that allow synthesis of proteins from mRNAS
3NP ITA MHA	2093604	TCGGCG	non coding transcript exon	serU	Regulation adapters that allow synthesis of proteins from MRNAS
ITA M9A	2093608	TCGGCG	non coding transcript exon	serU	Regulation adapters that allow synthesis of proteins from MRNAS
3NP M9A	2093615	A	non coding transcript exon	serU	Regulation adapters that allow synthesis of proteins from MRNAS
ITA MHA	2093620	CGCAA	non coding transcript exon	serU	Regulation adapters that allow synthesis of proteins from MRNAS
3NP ITA MHA 2093621	2093621	CGCAA	non coding transcript exon	serU	Regulation adapters that allow synthesis of proteins from MRNAS
ITA M9A	2093623	CGCAA	non coding transcript exon	serU	Regulation adapters that allow synthesis of proteins from MRNAS
3NP M9A	2093624	CGCAA	non coding transcript exon	serU	Regulation adapters that allow synthesis of proteins from MRNAS
3NP ITA MHA 2942387	2942387	A	missense	iroD	Enterochelin esterase activity, iron ion binding
ITA M9A	3804108	T	missense	dctA	Dicarboxylate/amino acid:cation symporter: Responsible for the transport of dicarboxylates such as succinate, fumarate, and malate from the periplasm across the membrane.

Figure 23: SNPs found in population samples.

As seen in figure 22, there were 12 total SNPs found in the clonal samples. Four of these were synonymous, while 8 SNPs were found to be nonsynonymous. The genes that were affected by these mutations revolved around RrT SRNA, cobyrinic acid synthase, cell division, RNA polymerase, flagella regulation, symporter, and nitrogen metabolism regulation. Similarly to the population samples, the affected genes were not related to 3NP or its function, indicating that there is no genetic selection against 3NP in the clonal samples.

One can also look at the balance between nonsynonymous and synonymous mutation as an indication for selection. It is expected that if there is genetic selection against 3NP, one would see more non synonymous mutations compared to synonymous. While, if there is no genetic selection against 3NP, it is expected that there would be more synonymous mutations compared to nonsynonymous. These findings were consistent in the population samples SNPs (Figure 21), but differed in the clonal samples (Figure 22). Although there were more non-synonymous mutations in the clonal samples, they were not related to 3NP function, thus no selection occurred.

Sample	POS	REF	ALT	NT_POS	TYPE OF MUTATION	FUNCTION
3NP-M9A	833062	T	C	804/1302	synonymous	Oxalacetate decarboxylase subunit beta
3NP-M9A	1863738	A	C		intragenic	RtT SRNA
ITA-M9A	1863738	A	C		intragenic	RtT SRNA
ITA-M9A	2152529	G	A	225/1521	synonymous	Cobyric acid synthase
ITA-M9A	3750799	CCAGCAGCAGC	CCAGCAGC	974/1056	conservative	Cell division protein FtsX
ITA-M9A	4380519	G	T	1031/4029	missense	DNA-directed RNA polymerase subunit beta
ITA-M9A	1433140	C	T	367/714	stop gained	Anti-FlhDC factor YdiV
ITA-M9A	3533039	A	G	891/1302	synonymous	Oxalacetate decarboxylase subunit beta
ITA-M9A	3750799	CCAGCAGCAGC	CCAGCAGC	974/1056	inframe deletion	Cell division protein FtsX
ITA-M9A	3804108	C	T	1150/1287	missense	Dicarboxylate/amino acid:cation symporter: Responsible for the transport of dicarboxylates such as succinate, fumarate, and malate from the periplasm across the membrane.
ITA-MHA	3180176	C	A	1789/2247	stop gained	Phosphoenolpyruvate-protein phosphotransferase PtsP
ITA-MHA	3533039	A	G	891/1302	synonymous	Oxalacetate decarboxylase subunit beta

Figure 24: SNPs found in clonal samples.

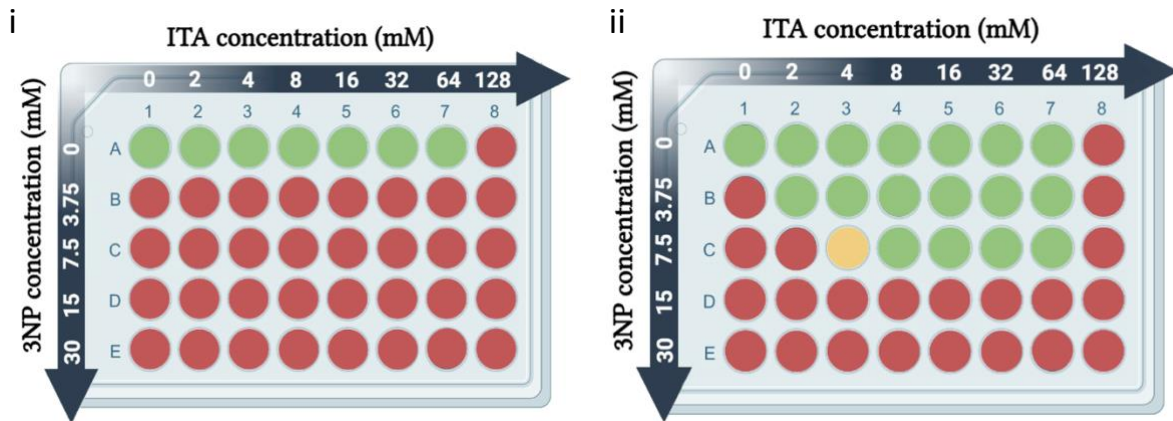


Figure 25: i) 3NP + ITA-naïve *S. Typhimurium* checkerboard ii) 3NP + ITA-resistant *S. Typhimurium* checkerboard. Green wells indicating full growth, yellow wells indicating partial growth, red wells indicating no growth.

Upon further study, it was found that 3NP exhibited antimicrobial activity at concentrations less than 3.75mM against both naïve and ITA-resistant *S. Typhimurium* (Figure 23). As seen in Figure 23 i, the MIC of ITA is 128 mM while the MIC of 3NP is 3.75 mM against naïve *S. Typhimurium* cells. The FIC was calculated to be 1, indicating additive interaction. The MIC of ITA against ITA-resistant *S. Typhimurium* cells is 128 mM and 3NP's MIC is 3.75 mM. While the FIC was calculated to be 1, indicating additive interaction. These results show that 3NP is antimicrobial at a low concentration of 3.75 mM. 3NP is therefore not a suitable adjuvant to pursue forward because selection against 3NP will occur faster than a compound with no antimicrobial activity.

Discussion:

In this study we screened a diverse library of 74 natural products against a small panel of *E. coli* MG1655 mutants that were individually resistant to 6 clinically-relevant antibiotics. From this preliminary screen we identified several compounds that were able to restore killing against the antibiotic-resistant cells, including one, perforone, which was effective only in combination with polymyxin B against the polymyxin B-resistant strain. Perforone allowed the passage of protons across inner membrane of *E. coli*, as measured by changes in the cytosolic pH of treated cells, behaviour that is likely to synergize with the pore-forming activity of polymyxin B.¹³¹

Antimicrobial resistance is a growing global public-health crisis, and new approaches to combat the rising tide of resistant bacteria are urgently needed. Mutations which provide resistance to antibiotics often reduce fitness along other axes,¹³⁹ and our results suggest that this vulnerability can be readily exploited. Aside from the positive control doxycycline, only one of the compounds in our panel was able to even partially inhibit the growth of *E. coli* MG1655, but 31% (23/74) of the compounds inhibited the growth of one or more of the resistant strains. This suggests that it may be possible to prolong the use of common antibiotics against even resistant bacteria, through the discovery of new antibiotic adjuvants.

A study by Song *et al.* performed a similar study targeting resistant Gram-negative bacteria through antibiotic adjuvants. They identified an antibacterial peptide, SLAP-S25 through a screen of short linear peptides. SLAP-25 exhibited weak antimicrobial activity, but

was able to resensitize multi-drug resistant Gram-negative bacteria to different antibiotic classes in three animal models. SLAP-25 functions by triggering membrane damage by binding to LPS in the outer membrane and phosphatidylglycerol (PG) in the cytoplasmic membrane. This study showed that drug modalities aside from small molecules can be effective as adjuvants in targeting resistant bacteria and potentiating antibiotic activity. The future prospects for perforone would be to test in animal models to obtain *in vivo* data, similarly to this study.¹⁴⁰

Investment from pharmaceutical companies to discover and develop antimicrobials has decreased¹⁴¹. This is because resistance emerges against the new antimicrobial causing it to fail in clinical trials or shortly after getting to market, so the investment is risky¹⁴¹. This narrative has started to change over the past decade. Emerging biotech companies are venturing in this space to specifically address resistant bacteria. For example, Bugworks Research is developing GYROX, a gyrase-topoisomerase inhibitor which targets resistant Gram-negative and Gram-positive bacteria. GYROX is currently in phase 1 clinical trials¹⁴². Alternative approaches such as adjuvant therapeutics show promise to combat antimicrobial resistance by prolonging resistance from occurring and increasing the shelf-life of antibiotics therapies. This could help de-risk the antibiotic development pipeline and entice pharmaceutical companies to continue developing novel therapeutics¹⁴¹.

The Pathogen Box screen strove to repurpose drug-like compounds for antimicrobial use against Gram-negative bacteria. A screen of the Pathogen Box compounds in combination with

EDTA was done to identify compounds that could inhibit the growth of Gram-negative bacteria. 33 compounds showed antimicrobial activity with EDTA against *E. coli* MG1655. 24 compounds passed QC using RP-LCMS, indicating that they were pure compounds. Four candidates were selected as leads to undergo analogue generation studies to add primary amines to the structures. Studies are currently underway to generate a panel of analogs that possess primary amines at various positions to see what increases accumulation into Gram-negative bacteria.

Gram-negative bacteria are notoriously more difficult to eradicate than Gram-positive bacteria due to their double-layered membrane composed of peptidoglycan and LPS making it difficult for compounds to enter and accumulate inside the cell¹⁴³. Richter *et. al.* identified key properties of compounds that are selectively active against Gram-positive bacteria⁹⁶. Adding a primary amine to compounds that have low globularity and low number of rotatable bonds have been linked to a higher likelihood to accumulate in Gram-negative bacteria⁹⁶.

Instead of focusing on structure-activity relationship (SAR) studies like the Richter *et. al.* accumulation study, we attempted a more empirical approach based on the results they obtained. We designed a high-throughput approach to find compounds that were active against Gram-negative bacteria if cell entry was facilitated using a chemical approach. Using EDTA we increased membrane permeability, which would allow us to discern promising antimicrobial compounds that could be tailored to become broad-spectrum. This approach is promising as we've shown that if we can get these compounds inside Gram-negative bacteria through the addition of primary amines we can eradicate Gram-negative bacteria. The results from this

work agree with the hypothesis that many compounds are effective against Gram-negative bacteria, but they are unable to enter the cell.

Recent studies screening the Pathogen Box identified compounds that are effective against *Toxoplasma gondii*, a protozoan parasite, and *Mycobacterium abscessus*, a Gram-positive bacteria^{144,145}. This approach can help speed up the drug development process since these compounds are already well characterized and tested for other therapeutic purposes¹⁹. However, no studies have repurposed Pathogen Box compounds as antimicrobials active against Gram-negative bacteria. My work successfully identified 24 compounds which could be repurposed for antimicrobial use against Gram-negative bacteria.

The Pathogen Box has also been repurposed towards anti-fungals. Vila *et al.*, screened the Pathogen Box for inhibitors of *Candida albicans* biofilm formation¹⁴⁶. They identified seven hits, three of which (MMV688768, MMV687273, and MMV687807) were able to target cells within preformed biofilms and decrease the metabolic activity. Their lead candidate with the most potent activity, MMV688768, exhibited increased activity against biofilms, compared to planktonic cells¹⁴⁶. This suggests that it may target processes involved with biofilm formation. This study highlights the potential for repurposing known and characterized compounds, and the diversity of the Pathogen Box. This also demonstrated the potential of Pathogen Box compounds as inhibitors of biofilms. Our future studies can involve screening the Pathogen Box for inhibitor of Gram-negative bacteria biofilm formation.

Drugs have been repurposed for other therapeutic areas in the past¹⁴⁷. For example, thalidomide, which was introduced in the 1950s to treat insomnia and morning sickness, is one such example¹⁴⁸. However, this drug was found to be extremely unsafe and was pulled from the clinic¹⁴⁸. Repurposed derivatives of thalidomide came to market in the 1960s to treat skin lesions and granulomas associated with leprosy¹⁴⁹. At present day, it is also used as a first-line treatment for Hansen's disease¹⁵⁰. The development and approval process for this was far less, since thalidomide was developed and tested for other therapeutic indications¹⁵⁰. Not all drugs are suitable for repurposing, especially if they have poor physicochemical issues and side effects. Optimizing derivatives of these drugs to have better side effect profiles is a suitable approach to mitigate this¹⁵¹. This example shows that repurposing drugs can work for various therapeutic purposes and decrease the amount of time needed to get a drug to the clinic.

There are still 18 Pathogen Box candidates that exhibited good activity against *E. coli* MG1655 in combination with EDTA that haven't been selected for analogue generation and optimization. Many of these have an ideal backbone structure and physicochemical properties for amine addition and structure optimization. Future work will involve further characterization on these compounds and mechanistic studies to understand how they function. The Pathogen Box approach could also be applied to perforone. We can create analogs of perforone and optimize its structure to see if its activity improves. Gram-negative infections continue to rise in prevalence in the clinical setting. More compounds that specifically eradicate Gram-negative bacteria must continue to be discovered and developed.

To truly understand how antimicrobial resistance functions, one must look at bacteria from the genomic level. This study set out to characterize bacterio-modulation at the genetic level, specifically by looking at the evolution of resistance against ITA and 3NP. To do this, cells were run through SAGE plates with variable concentrations of ITA and 3NP and types of media. Population and clonal samples were collected from the end of the SAGE plates and sent for Illumina Shotgun sequencing. The sequencing data was analyzed using a bioinformatics approach and SNPs were analyzed. It was found that there was no genetic selection against 3NP.

However, it was also uncovered during this work that 3NP is antimicrobial against *S. Typhimurium* at 3.75 mM. One hypothesis as to why no genetic selection was seen against 3NP is that the population and clonal samples were heteroresistant. These bacteria are composed of heterogeneous subpopulations of susceptible and resistant bacteria¹⁵². The resistant bacteria in these populations tend to be genetically unstable due to tandem amplification of resistance genes. This is observed for *S. Typhimurium* when amplification of the *bla*TEM-1B gene results in heteroresistant cells against cephalothin¹⁵³. The same phenomenon is observed for Polymyxin-resistant subpopulations that show increased expression levels of *PhoPQ* and *pmrD*, which are part of the two-component system that leads to LPS modification in Gram-negative bacteria^{154,155}. Heteroresistance has been found to be very common amongst different bacterial species and antibiotics¹⁵³. For example, Andersson *et al.*, tested 766 bacteria-antibiotic combinations and found as much 27.4% of the total were heteroresistant¹⁵³. In the absence of antibiotics, the subpopulation of resistant cells revert back to a susceptible state. This could

explain our results as the population and clonal samples were not kept in the presence of 3NP and ITA during sample extractions, and therefore could have reverted back to susceptibility.

This is a promising result as it indicates that adjuvant compounds can help prolong resistance from occurring since there is no genetic selection against them. If 3NP was posing a selective pressure on *S. Typhimurium* then SNPs related to 3NP function would have been found. This was seen in a study by Kim *et al.* that studied SNPs in a vancomycin-resistant *Staphylococcus aureus* strain. Whole-genome sequencing revealed that the resistant bacteria possessed eight SNPs related to cell wall synthesis. Additionally, morphologically the cells had a twofold thicker cell wall. This resistant mechanism makes sense since vancomycin functions by inhibiting cell wall synthesis¹⁵⁶.

This phenomenon was observed with co-amoxiclav, a combination of the antibiotic amoxicillin, and adjuvant clavulanate. Although resistance was eventually observed over time, it was found that by fine-tuning the adjuvant to antibiotic ratio, with higher adjuvant concentrations, the evolution of resistance can be steered and slowed⁴³. These principles should be taken more into account in the clinical setting and when prescribing antibiotic and adjuvant regimens.

3NP will no longer be pursued as an adjuvant as it was found to be antimicrobial at concentrations less than 3.75 mM. In order to deter bacterial selection against an adjuvant and prolong resistance from occurring, adjuvants should have little to no antimicrobial activity. One

example of this is phenylalanine-arginine- β -naphthylamide (PA β N), an efflux pump inhibitor which potentiates the activity of fluorquinolones and beta lactam antibiotics. Pa β N functions specifically on the RND efflux pump family by restraining drug-binding pocket dynamics, preventing it from pumping out the antibiotics. Pa β N doesn't possess any antimicrobial activity, it only potentiates the activity of the antibiotics to function¹⁵⁷. This may prolong resistance from occurring against Pa β N.

This thesis strove to combat antimicrobial resistance through the discovery of adjuvants that could resensitize resistant bacteria to antibiotics, repurpose drug-like compounds for antimicrobial use against Gram-negative, and understand resistance emergence through analyzing SNPs. These three approaches can be combined to help in the fight against antimicrobial resistance. By understanding how resistance emerges at the genetic level, we can select specific resistant genes to screen for in order to identify antibiotic adjuvants. We can then generate analogs and optimize the lead structure in an effort to push it down the development pipeline and ultimately treat patients.

References

1. Murray, C. J. *et al.* Global burden of bacterial antimicrobial resistance in 2019: a systematic analysis. *The Lancet* **399**, 629–655 (2022).
2. Laxminarayan, R. *et al.* Antibiotic resistance—the need for global solutions. *Lancet Infect. Dis.* **13**, 1057–1098 (2013).
3. Adedeji, W. A. THE TREASURE CALLED ANTIBIOTICS. *Ann. Ib. Postgrad. Med.* **14**, 56–57 (2016).
4. Kupferschmidt, K. Resistance fighters. *Science* **352**, 758–761 (2016).
5. Lobanovska, M. & Pilla, G. Penicillin’s Discovery and Antibiotic Resistance: Lessons for the Future? *Yale J. Biol. Med.* **90**, 135–145 (2017).
6. Chung, H. *et al.* Rapid expansion and extinction of antibiotic resistance mutations during treatment of acute bacterial respiratory infections. *Nat. Commun.* **13**, 1231 (2022).
7. O’Dwyer, K. *et al.* Bacterial Resistance to Leucyl-tRNA Synthetase Inhibitor GSK2251052 Develops during Treatment of Complicated Urinary Tract Infections. *Antimicrob. Agents Chemother.* **59**, 289–298 (2015).
8. Payne, D. J., Gwynn, M. N., Holmes, D. J. & Pompliano, D. L. Drugs for bad bugs: confronting the challenges of antibacterial discovery. *Nat. Rev. Drug Discov.* **6**, 29–40 (2007).
9. Reygaert, W. C. An overview of the antimicrobial resistance mechanisms of bacteria. *AIMS Microbiol.* **4**, 482–501 (2018).
10. Sun, D., Jeannot, K., Xiao, Y. & Knapp, C. W. Editorial: Horizontal Gene Transfer Mediated Bacterial Antibiotic Resistance. *Front. Microbiol.* **10**, (2019).

11. Courvalin, P. New plasmid-mediated resistances to antimicrobial agents. *Arch. Microbiol.* **189**, 289–291 (2008).
12. Pribis, J. P. *et al.* Gamblers: an Antibiotic-induced Evolvable Cell Subpopulation Differentiated by Reactive-oxygen-induced General Stress Response. *Mol. Cell* **74**, 785–800.e7 (2019).
13. Kohanski, M. A., DePristo, M. A. & Collins, J. J. Sublethal antibiotic treatment leads to multidrug resistance via radical-induced mutagenesis. *Mol. Cell* **37**, 311–320 (2010).
14. Børsting, C. & Morling, N. Single-Nucleotide Polymorphisms. in *Encyclopedia of Forensic Sciences (Second Edition)* (eds. Siegel, J. A., Saukko, P. J. & Houck, M. M.) 233–238 (Academic Press, 2013). doi:10.1016/B978-0-12-382165-2.00042-8.
15. Hunt, R., Sauna, Z. E., Ambudkar, S. V., Gottesman, M. M. & Kimchi-Sarfaty, C. Silent (Synonymous) SNPs: Should We Care About Them? in *Single Nucleotide Polymorphisms: Methods and Protocols* (ed. Komar, A. A.) 23–39 (Humana Press, 2009). doi:10.1007/978-1-60327-411-1_2.
16. Ramanathan, B. *et al.* Next generation sequencing reveals the antibiotic resistant variants in the genome of *Pseudomonas aeruginosa*. *PLoS ONE* **12**, e0182524 (2017).
17. Blair, J. M. A., Webber, M. A., Baylay, A. J., Ogbolu, D. O. & Piddock, L. J. V. Molecular mechanisms of antibiotic resistance. *Nat. Rev. Microbiol.* **13**, 42–51 (2015).
18. Cochrane, S. A. *et al.* Antimicrobial lipopeptide tridecaptin A1 selectively binds to Gram-negative lipid II. *Proc. Natl. Acad. Sci. U. S. A.* **113**, 11561–11566 (2016).
19. Cochrane, S. A. *et al.* Antimicrobial lipopeptide tridecaptin A1 selectively binds to Gram-negative lipid II. *Proc. Natl. Acad. Sci.* **113**, 11561–11566 (2016).

20. Lee, M. & Sousa, M. C. Structural basis for substrate specificity in ArnB. A key enzyme in the polymyxin resistance pathway of Gram-negative bacteria. *Biochemistry* **53**, 796–805 (2014).
21. Arroyo, L. A. *et al.* The pmrCAB Operon Mediates Polymyxin Resistance in *Acinetobacter baumannii* ATCC 17978 and Clinical Isolates through Phosphoethanolamine Modification of Lipid A. *Antimicrob. Agents Chemother.* **55**, 3743–3751 (2011).
22. Gomes, C., Ruiz-Roldán, L., Mateu, J., Ochoa, T. J. & Ruiz, J. Azithromycin resistance levels and mechanisms in *Escherichia coli*. *Sci. Rep.* **9**, 6089 (2019).
23. Heidary, M. *et al.* Mechanism of action, resistance, synergism, and clinical implications of azithromycin. *J. Clin. Lab. Anal.* **36**, e24427 (2022).
24. Eliopoulos, G. M. & Huovinen, P. Resistance to Trimethoprim-Sulfamethoxazole. *Clin. Infect. Dis.* **32**, 1608–1614 (2001).
25. Sanders, C. C. Ciprofloxacin: In Vitro Activity, Mechanism of Action, and Resistance. *Rev. Infect. Dis.* **10**, 516–527 (1988).
26. Qin, T.-T. *et al.* SOS response and its regulation on the fluoroquinolone resistance. *Ann. Transl. Med.* **3**, 358–358 (2015).
27. Grossman, T. H. Tetracycline Antibiotics and Resistance. *Cold Spring Harb. Perspect. Med.* **6**, a025387 (2016).
28. Castro, R. A. D. *et al.* The Genetic Background Modulates the Evolution of Fluoroquinolone-Resistance in *Mycobacterium tuberculosis*. *Mol. Biol. Evol.* **37**, 195–207 (2020).
29. Bui, T. & Preuss, C. V. Cephalosporins. in *StatPearls* (StatPearls Publishing, 2022).

30. Fischer, M. A. *et al.* Population structure-guided profiling of antibiotic resistance patterns in clinical *Listeria monocytogenes* isolates from Germany identifies pbpB3 alleles associated with low levels of cephalosporin resistance. *Emerg. Microbes Infect.* **9**, 1804–1813.
31. Guinane, C. M., Cotter, P. D., Ross, R. P. & Hill, C. Contribution of Penicillin-Binding Protein Homologs to Antibiotic Resistance, Cell Morphology, and Virulence of *Listeria monocytogenes* EGDe. *Antimicrob. Agents Chemother.* **50**, 2824–2828 (2006).
32. Breijyeh, Z., Jubeh, B. & Karaman, R. Resistance of Gram-Negative Bacteria to Current Antibacterial Agents and Approaches to Resolve It. *Molecules* **25**, 1340 (2020).
33. Oliveira, J. & Reygaert, W. C. Gram Negative Bacteria. in *StatPearls* (StatPearls Publishing, 2022).
34. Choi, U. & Lee, C.-R. Distinct Roles of Outer Membrane Porins in Antibiotic Resistance and Membrane Integrity in *Escherichia coli*. *Front. Microbiol.* **10**, 953 (2019).
35. Gottlieb, D. & Shaw, P. D. *Antibiotics: Volume I Mechanism of Action*. (Springer, 2013).
36. Rosas, N. C. & Lithgow, T. Targeting bacterial outer-membrane remodelling to impact antimicrobial drug resistance. *Trends Microbiol.* **30**, 544–552 (2022).
37. Zulauf, K. E. & Kirby, J. E. Discovery of small-molecule inhibitors of multidrug-resistance plasmid maintenance using a high-throughput screening approach. *Proc. Natl. Acad. Sci. U. S. A.* **117**, 29839–29850 (2020).
38. Walkty, A. *et al.* Antimicrobial susceptibility of 2906 *Pseudomonasaeruginosa* clinical isolates obtained from patients in Canadian hospitals over a period of 8 years: Results of the Canadian Ward surveillance study (CANWARD), 2008-2015. *Diagn. Microbiol. Infect. Dis.* **87**, 60–63 (2017).

39. Zhanel, G. G. *et al.* 42936 Pathogens from Canadian hospitals: 10 years of results (2007-16) from the CANWARD surveillance study. *J. Antimicrob. Chemother.* **74**, (2019).
40. Dewachter, L., Fauvart, M. & Michiels, J. Bacterial Heterogeneity and Antibiotic Survival: Understanding and Combatting Persistence and Heteroresistance. *Mol. Cell* **76**, 255–267 (2019).
41. Gould, I. M. *et al.* New insights into methicillin-resistant *Staphylococcus aureus* (MRSA) pathogenesis, treatment and resistance. *Int. J. Antimicrob. Agents* **39**, 96–104 (2012).
42. Sholeh, M. *et al.* Antimicrobial resistance in *Clostridioides (Clostridium) difficile* derived from humans: a systematic review and meta-analysis. *Antimicrob. Resist. Infect. Control* **9**, 158 (2020).
43. Allen, R. C. & Brown, S. P. Modified Antibiotic Adjuvant Ratios Can Slow and Steer the Evolution of Resistance: Co-amoxiclav as a Case Study. *mBio* **10**, e01831-19 (2019).
44. Wright, G. D. Antibiotic Adjuvants: Rescuing Antibiotics from Resistance. *Trends Microbiol.* **24**, 862–871 (2016).
45. Liu, Y., Li, R., Xiao, X. & Wang, Z. Antibiotic adjuvants: an alternative approach to overcome multi-drug resistant Gram-negative bacteria. *Crit. Rev. Microbiol.* **45**, 301–314 (2019).
46. Bengtsson, T. *et al.* Plantaricin NC8 $\alpha\beta$ exerts potent antimicrobial activity against *Staphylococcus* spp. and enhances the effects of antibiotics. *Sci. Rep.* **10**, 3580 (2020).
47. Sjuts, H. *et al.* Molecular basis for inhibition of AcrB multidrug efflux pump by novel and powerful pyranopyridine derivatives. *Proc. Natl. Acad. Sci.* **113**, 3509–3514 (2016).

48. Rogers, S. A., Huigens, R. W., Cavanagh, J. & Melander, C. Synergistic Effects between Conventional Antibiotics and 2-Aminoimidazole-Derived Antibiofilm Agents. *Antimicrob. Agents Chemother.* **54**, 2112–2118 (2010).
49. Perry, J. A. *et al.* A macrophage-stimulating compound from a screen of microbial natural products. *J. Antibiot. (Tokyo)* **68**, 40–46 (2015).
50. Audi, S. *et al.* The ‘top 100’ drugs and classes in England: an updated ‘starter formulary’ for trainee prescribers. *Br. J. Clin. Pharmacol.* **84**, 2562–2571 (2018).
51. Oteo, J. *et al.* Increased Amoxicillin–Clavulanic Acid Resistance in Escherichia coli Blood Isolates, Spain. *Emerg. Infect. Dis.* **14**, 1259–1262 (2008).
52. P, S. *et al.* Incidence and mechanisms of resistance to the combination of amoxicillin and clavulanic acid in Escherichia coli. *Antimicrob. Agents Chemother.* **39**, (1995).
53. Lenski, R. E., Rose, M. R., Simpson, S. C. & Tadler, S. C. Long-Term Experimental Evolution in Escherichia coli. I. Adaptation and Divergence During 2,000 Generations. *Am. Nat.* **138**, 1315–1341 (1991).
54. Toprak, E. *et al.* Building a morbidostat: an automated continuous-culture device for studying bacterial drug resistance under dynamically sustained drug inhibition. *Nat. Protoc.* **8**, 555–567 (2013).
55. Baym, M. *et al.* Spatiotemporal microbial evolution on antibiotic landscapes. *Science* **353**, 1147–1151 (2016).
56. Toprak, E. *et al.* Evolutionary paths to antibiotic resistance under dynamically sustained drug selection. *Nat. Genet.* **44**, 101–105 (2011).

57. Spagnolo, F., Rinaldi, C., Sajorda, D. R. & Dykhuizen, D. E. Evolution of Resistance to Continuously Increasing Streptomycin Concentrations in Populations of *Escherichia coli*. *Antimicrob. Agents Chemother.* **60**, 1336–1342 (2016).
58. Wadhams, G. H. & Armitage, J. P. Making sense of it all: bacterial chemotaxis. *Nat. Rev. Mol. Cell Biol.* **5**, 1024–1037 (2004).
59. Ghaddar, N., Hashemidahaj, M. & Findlay, B. L. Access to high-impact mutations constrains the evolution of antibiotic resistance in soft agar. *Sci. Rep.* **8**, 17023 (2018).
60. Bennett, P. M. Plasmid encoded antibiotic resistance: acquisition and transfer of antibiotic resistance genes in bacteria. *Br. J. Pharmacol.* **153**, S347–S357 (2008).
61. Munita, J. M. & Arias, C. A. Mechanisms of Antibiotic Resistance. *Microbiol. Spectr.* **4**, 4.2.15 (2016).
62. Szybalski, W. & Bryson, V. GENETIC STUDIES ON MICROBIAL CROSS RESISTANCE TO TOXIC AGENTS I. ,. *J. Bacteriol.* **64**, 489–499 (1952).
63. Rathinakumar, R. & Wimley, W. C. High-throughput discovery of broad-spectrum peptide antibiotics. *FASEB J.* **24**, 3232–3238 (2010).
64. Lewis, K. Platforms for antibiotic discovery. *Nat. Rev. Drug Discov.* **12**, 371–387 (2013).
65. Hertzberg, R. P. & Pope, A. J. High-throughput screening: new technology for the 21st century. *Curr. Opin. Chem. Biol.* **4**, 445–451 (2000).
66. Taylor, P. L., Rossi, L., De Pascale, G. & Wright, G. D. A forward chemical screen identifies antibiotic adjuvants in *Escherichia coli*. *ACS Chem. Biol.* **7**, 1547–1555 (2012).
67. Broach, J. R. & Thorner, J. High-throughput screening for drug discovery. *Nature* **384**, 14–16 (1996).

68. Carnero, A. High throughput screening in drug discovery. *Clin. Transl. Oncol.* **8**, 482–490 (2006).
69. Wiegand, I., Hilpert, K. & Hancock, R. E. W. Agar and broth dilution methods to determine the minimal inhibitory concentration (MIC) of antimicrobial substances. *Nat. Protoc.* **3**, 163–175 (2008).
70. Kowalska-Krochmal, B. & Dudek-Wicher, R. The Minimum Inhibitory Concentration of Antibiotics: Methods, Interpretation, Clinical Relevance. *Pathogens* **10**, 165 (2021).
71. Zhu, M., Tse, M. W., Weller, J., Chen, J. & Blainey, P. C. The future of antibiotics begins with discovering new combinations. *Ann. N. Y. Acad. Sci.* **1496**, 82–96 (2021).
72. Tan, T. Y. *et al.* In Vitro Antibiotic Synergy in Extensively Drug-Resistant *Acinetobacter baumannii*: the Effect of Testing by Time-Kill, Checkerboard, and Etest Methods. *Antimicrob. Agents Chemother.* **55**, 436–438 (2011).
73. Orhan, G., Bayram, A., Zer, Y. & Balci, I. Synergy Tests by E Test and Checkerboard Methods of Antimicrobial Combinations against *Brucella melitensis*. *J. Clin. Microbiol.* **43**, 140–143 (2005).
74. Doern, C. D. When Does 2 Plus 2 Equal 5? A Review of Antimicrobial Synergy Testing. *J. Clin. Microbiol.* **52**, 4124–4128 (2014).
75. Meletiadis, J., Pournaras, S., Roilides, E. & Walsh, T. J. Defining fractional inhibitory concentration index cutoffs for additive interactions based on self-drug additive combinations, Monte Carlo simulation analysis, and in vitro-in vivo correlation data for antifungal drug combinations against *Aspergillus fumigatus*. *Antimicrob. Agents Chemother.* **54**, 602–609 (2010).

76. den Hollander, J. G., Mouton, J. W. & Verbrugh, H. A. Use of Pharmacodynamic Parameters To Predict Efficacy of Combination Therapy by Using Fractional Inhibitory Concentration Kinetics. *Antimicrob. Agents Chemother.* **42**, 744–748 (1998).
77. Konaté, K. *et al.* Antibacterial activity against β -lactamase producing Methicillin and Ampicillin-resistant Staphylococcus aureus: fractional Inhibitory Concentration Index (FICI) determination. *Ann. Clin. Microbiol. Antimicrob.* **11**, 18 (2012).
78. Li, R. C., Schentag, J. J. & Nix, D. E. The fractional maximal effect method: a new way to characterize the effect of antibiotic combinations and other nonlinear pharmacodynamic interactions. *Antimicrob. Agents Chemother.* **37**, 523–531 (1993).
79. Prichard, M. N. & Shipman, C. A three-dimensional model to analyze drug-drug interactions. *Antiviral Res.* **14**, 181–205 (1990).
80. Pandey, N. & Cascella, M. Beta Lactam Antibiotics. in *StatPearls* (StatPearls Publishing, 2022).
81. Krishnamurthy, M. *et al.* Enhancing the antibacterial activity of polymyxins using a nonantibiotic drug. *Infect. Drug Resist.* **12**, 1393–1405 (2019).
82. Biswas, S., Brunel, J.-M., Dubus, J.-C., Reynaud-Gaubert, M. & Rolain, J.-M. Colistin: an update on the antibiotic of the 21st century. *Expert Rev. Anti Infect. Ther.* **10**, 917–934 (2012).
83. Cannatelli, A. *et al.* In Vivo Emergence of Colistin Resistance in Klebsiella pneumoniae Producing KPC-Type Carbapenemases Mediated by Insertional Inactivation of the PhoQ/PhoP mgrB Regulator. *Antimicrob. Agents Chemother.* **57**, 5521–5526 (2013).

84. Phan, M.-D. *et al.* Modifications in the pmrB gene are the primary mechanism for the development of chromosomally encoded resistance to polymyxins in uropathogenic *Escherichia coli*. *J. Antimicrob. Chemother.* **72**, 2729–2736 (2017).
85. Berrocal-Lobo, M., Molina, A., Rodríguez-Palenzuela, P., García-Olmedo, F. & Rivas, L. *Leishmania donovani*: Thionins, plant antimicrobial peptides with leishmanicidal activity. *Exp. Parasitol.* **122**, 247–249 (2009).
86. Zhang, L., Dhillon, P., Yan, H., Farmer, S. & Hancock, R. E. W. Interactions of Bacterial Cationic Peptide Antibiotics with Outer and Cytoplasmic Membranes of *Pseudomonas aeruginosa*. *Antimicrob. Agents Chemother.* **44**, 3317–3321 (2000).
87. Hancock, R. E. W. & Rozek, A. Role of membranes in the activities of antimicrobial cationic peptides. *FEMS Microbiol. Lett.* **206**, 143–149 (2002).
88. Boix-Lemonche, G., Lekka, M. & Skerlavaj, B. A Rapid Fluorescence-Based Microplate Assay to Investigate the Interaction of Membrane Active Antimicrobial Peptides with Whole Gram-Positive Bacteria. *Antibiotics* **9**, 92 (2020).
89. Aono, R., Ito, M. & Horikoshi, K. 1997. Measurement of cytoplasmic pH of the alkaliphile *Bacillus lentus* C-125 with a fluorescent pH probe. *Microbiology* **143**, 2531–2536.
90. Molenaar, D., Abee, T. & Konings, W. N. Continuous measurement of the cytoplasmic pH in *Lactococcus lactis* with a fluorescent pH indicator. *Biochim. Biophys. Acta BBA - Gen. Subj.* **1115**, 75–83 (1991).
91. Villanueva, J. A. *et al.* *Salmonella enterica* Infections Are Disrupted by Two Small Molecules That Accumulate within Phagosomes and Differentially Damage Bacterial Inner Membranes. *mBio* **13**, e01790-22 (2022).

92. Stark, G. & Benz, R. The transport of potassium through lipid bilayer membranes by the neutral carriers valinomycin and monactin. *J. Membr. Biol.* **5**, 133–153 (1971).
93. Liu, Y. *et al.* Drug repurposing for next-generation combination therapies against multidrug-resistant bacteria. *Theranostics* **11**, 4910–4928 (2021).
94. Veale, C. G. L. Unpacking the Pathogen Box-An Open Source Tool for Fighting Neglected Tropical Disease. *ChemMedChem* **14**, 386–453 (2019).
95. About the Pathogen Box | Medicines for Malaria Venture. <https://www.mmv.org/mmv-open/pathogen-box/about-pathogen-box>.
96. Richter, M. F. *et al.* Predictive compound accumulation rules yield a broad-spectrum antibiotic. *Nature* **545**, 299–304 (2017).
97. Prajapati, J. D., Kleinekathöfer, U. & Winterhalter, M. How to Enter a Bacterium: Bacterial Porins and the Permeation of Antibiotics. *Chem. Rev.* **121**, 5158–5192 (2021).
98. Schulz, G. E. Bacterial porins: structure and function. *Curr. Opin. Cell Biol.* **5**, 701–707 (1993).
99. Markus, A. C. & Spencer, A. G. Treatment of Chronic Lead-poisoning with Calcium Disodium Versenate. *Br. Med. J.* **2**, 883–885 (1955).
100. Clarke, N. E., Clarke, C. N. & Mosher, R. E. The in vivo dissolution of metastatic calcium; an approach to atherosclerosis. *Am. J. Med. Sci.* **229**, 142–149 (1955).
101. Clarke, C. N., Clarke, N. E. & Mosher, R. E. Treatment of angina pectoris with disodium ethylene diamine tetraacetic acid. *Am. J. Med. Sci.* **232**, 654–666 (1956).

102. Chaudhary, M. & Payasi, A. Clinical, microbial efficacy and tolerability of Elores, a novel antibiotic adjuvant entity in ESBL producing pathogens: Prospective randomized controlled clinical trial. *J. Pharm. Res.* **7**, 275–280 (2013).
103. Goldschmidt, M. C. & Wyss, O. The role of tris in EDTA toxicity and lysozyme lysis. *J. Gen. Microbiol.* **47**, 421–431 (1967).
104. Nikaido, H. Molecular Basis of Bacterial Outer Membrane Permeability Revisited. *Microbiol. Mol. Biol. Rev.* **67**, 593–656 (2003).
105. Pelletier, C., Bourlioux, P. & van Heijenoort, J. Effects of sub-minimal inhibitory concentrations of EDTA on growth of *Escherichia coli* and the release of lipopolysaccharide. *FEMS Microbiol. Lett.* **117**, 203–206 (1994).
106. Umerska, A. *et al.* Synergistic Effect of Combinations Containing EDTA and the Antimicrobial Peptide AA230, an Arenicin-3 Derivative, on Gram-Negative Bacteria. *Biomolecules* **8**, (2018).
107. Salmonella Homepage | CDC. <https://www.cdc.gov/salmonella/index.html> (2022).
108. Takemura, R. & Werb, Z. Secretory products of macrophages and their physiological functions. *Am. J. Physiol.* **246**, C1-9 (1984).
109. Höner Zu Bentrup, K., Miczak, A., Swenson, D. L. & Russell, D. G. Characterization of activity and expression of isocitrate lyase in *Mycobacterium avium* and *Mycobacterium tuberculosis*. *J. Bacteriol.* **181**, 7161–7167 (1999).
110. Kornberg, H. L. The role and control of the glyoxylate cycle in *Escherichia coli*. *Biochem. J.* **99**, 1–11 (1966).

111. Hammerer, F., Chang, J. H., Duncan, D., Castañeda Ruiz, A. & Auclair, K. Small Molecule Restores Itaconate Sensitivity in *Salmonella enterica*: A Potential New Approach to Treating Bacterial Infections. *Chembiochem Eur. J. Chem. Biol.* **17**, 1513–1517 (2016).
112. Strelko, C. L. *et al.* Itaconic acid is a mammalian metabolite induced during macrophage activation. *J. Am. Chem. Soc.* **133**, 16386–16389 (2011).
113. Levy, S. E. & Myers, R. M. Advancements in Next-Generation Sequencing. *Annu. Rev. Genomics Hum. Genet.* **17**, 95–115 (2016).
114. Salipante, S. J. *et al.* Performance Comparison of Illumina and Ion Torrent Next-Generation Sequencing Platforms for 16S rRNA-Based Bacterial Community Profiling. *Appl. Environ. Microbiol.* **80**, 7583–7591 (2014).
115. Quail, M. A. *et al.* A large genome center's improvements to the Illumina sequencing system. *Nat. Methods* **5**, 1005–1010 (2008).
116. Sequencing-by-Synthesis: Explaining the Illumina Sequencing Technology. <https://bitesizebio.com/13546/sequencing-by-synthesis-explaining-the-illumina-sequencing-technology/> (2012).
117. Bankevich, A. *et al.* SPAdes: a new genome assembly algorithm and its applications to single-cell sequencing. *J. Comput. Biol. J. Comput. Mol. Cell Biol.* **19**, 455–477 (2012).
118. Gurevich, A., Saveliev, V., Vyahhi, N. & Tesler, G. QUAST: quality assessment tool for genome assemblies. *Bioinforma. Oxf. Engl.* **29**, 1072–1075 (2013).
119. Seemann, T. Snippy. (2022).
120. Backman, T. W. H., Cao, Y. & Girke, T. ChemMine tools: an online service for analyzing and clustering small molecules. *Nucleic Acids Res.* **39**, W486-491 (2011).

121. Shirai, K. & Matsuoka, M. Structure and properties of hematein derivatives. *Dyes Pigments* **32**, 159–169 (1996).
122. HUNG, M.-S. *et al.* Hematein, a casein kinase II inhibitor, inhibits lung cancer tumor growth in a murine xenograft model. *Int. J. Oncol.* **43**, 1517–1522 (2013).
123. Xu, H.-X. & Lee, S. F. The antibacterial principle of *Caesalpinia sappan*. *Phytother. Res. PTR* **18**, 647–651 (2004).
124. Amin, M. U., Khurram, M., Khattak, B. & Khan, J. Antibiotic additive and synergistic action of rutin, morin and quercetin against methicillin resistant *Staphylococcus aureus*. *BMC Complement. Altern. Med.* **15**, 59 (2015).
125. Arima, H., Ashida, H. & Danno, G. Rutin-enhanced antibacterial activities of flavonoids against *Bacillus cereus* and *Salmonella enteritidis*. *Biosci. Biotechnol. Biochem.* **66**, 1009–1014 (2002).
126. Peng, L.-Y. *et al.* Rutin inhibits quorum sensing, biofilm formation and virulence genes in avian pathogenic *Escherichia coli*. *Microb. Pathog.* **119**, 54–59 (2018).
127. Wu, T. *et al.* A structure–activity relationship study of flavonoids as inhibitors of *E. coli* by membrane interaction effect. *Biochim. Biophys. Acta BBA - Biomembr.* **1828**, 2751–2756 (2013).
128. Saidkhodzhaev, A. I. & Malikov, V. M. Structure of ugaferin and some properties of ugamdiol derivatives. *Chem. Nat. Compd.* **14**, 614–616 (1978).
129. Hall, M. J., Middleton, R. F. & Westmacott, D. The fractional inhibitory concentration (FIC) index as a measure of synergy. *J. Antimicrob. Chemother.* **11**, 427–433 (1983).

130. Tsubery, H., Ofek, I., Cohen, S. & Fridkin, M. Structure-function studies of polymyxin B nonapeptide: implications to sensitization of gram-negative bacteria. *J. Med. Chem.* **43**, 3085–3092 (2000).
131. H, T., I, O., S, C. & M, F. Structure-function studies of polymyxin B nonapeptide: implications to sensitization of gram-negative bacteria. *J. Med. Chem.* **43**, (2000).
132. Bessonova, I. A. Acetylhaplophyllidine, a new alkaloid from *Haplophyllum perforatum*. *Chem. Nat. Compd.* **35**, 589–590 (1999).
133. da Silva, H. C. *et al.* Structural characterization, antibacterial activity and NorA efflux pump inhibition of flavonoid fisetinidol. *South Afr. J. Bot.* **132**, 140–145 (2020).
134. Boualia, I. *et al.* Synthesis of novel 3-(quinazol-2-yl)-quinolines via SNAr and aluminum chloride-induced (hetero) arylation reactions and biological evaluation as proteasome inhibitors. *Tetrahedron Lett.* **61**, 151805 (2020).
135. Zhang, B., Liu, Z., Xia, S., Liu, Q. & Gou, S. Design, synthesis and biological evaluation of sulfamoylphenyl-quinazoline derivatives as potential EGFR/CAIX dual inhibitors. *Eur. J. Med. Chem.* **216**, 113300 (2021).
136. Hubbard, A. T. M. *et al.* Mechanism of Action of a Membrane-Active Quinoline-Based Antimicrobial on Natural and Model Bacterial Membranes. *Biochemistry* **56**, 1163–1174 (2017).
137. Insuasty, D. *et al.* Antimicrobial Activity of Quinoline-Based Hydroxyimidazolium Hybrids. *Antibiotics* **8**, 239 (2019).
138. Sohel, A. J., Shutter, M. C. & Molla, M. Fluoxetine. in *StatPearls* (StatPearls Publishing, 2022).

139. Melnyk, A. H., Wong, A. & Kassen, R. The fitness costs of antibiotic resistance mutations. *Evol. Appl.* **8**, 273–283 (2015).
140. Song, M. *et al.* A broad-spectrum antibiotic adjuvant reverses multidrug-resistant Gram-negative pathogens. *Nat. Microbiol.* **5**, 1040–1050 (2020).
141. Plackett, B. Why big pharma has abandoned antibiotics. *Nature* **586**, S50–S52 (2020).
142. qiworks. Pipeline. *Bugworks* <https://bugworksresearch.com/pipeline/> (2021).
143. MacVane, S. H. Antimicrobial Resistance in the Intensive Care Unit: A Focus on Gram-Negative Bacterial Infections. *J. Intensive Care Med.* **32**, 25–37 (2017).
144. Spalenka, J. *et al.* Discovery of New Inhibitors of *Toxoplasma gondii* via the Pathogen Box. *Antimicrob. Agents Chemother.* **62**, e01640-17 (2018).
145. Jeong, J. *et al.* Pathogen Box screening for hit identification against *Mycobacterium abscessus*. *PLOS ONE* **13**, e0195595 (2018).
146. Vila, T. & Lopez-Ribot, J. L. Screening the Pathogen Box for Identification of *Candida albicans* Biofilm Inhibitors. *Antimicrob. Agents Chemother.* **61**, e02006-16 (2016).
147. Sahoo, B. M. *et al.* Drug Repurposing Strategy (DRS): Emerging Approach to Identify Potential Therapeutics for Treatment of Novel Coronavirus Infection. *Front. Mol. Biosci.* **8**, (2021).
148. Kim, J. H. & Scialli, A. R. Thalidomide: the tragedy of birth defects and the effective treatment of disease. *Toxicol. Sci. Off. J. Soc. Toxicol.* **122**, 1–6 (2011).
149. Vargesson, N. Thalidomide-induced teratogenesis: History and mechanisms. *Birth Defects Res.* **105**, 140–156 (2015).

150. Rehman, W., Arfons, L. M. & Lazarus, H. M. The Rise, Fall and Subsequent Triumph of Thalidomide: Lessons Learned in Drug Development. *Ther. Adv. Hematol.* **2**, 291–308 (2011).
151. Schein, C. H. Repurposing approved drugs on the pathway to novel therapies. *Med. Res. Rev.* **40**, 586–605 (2020).
152. Andersson, D. I., Nicoloff, H. & Hjort, K. Mechanisms and clinical relevance of bacterial heteroresistance. *Nat. Rev. Microbiol.* **17**, 479–496 (2019).
153. Nicoloff, H., Hjort, K., Levin, B. R. & Andersson, D. I. The high prevalence of antibiotic heteroresistance in pathogenic bacteria is mainly caused by gene amplification. *Nat. Microbiol.* **4**, 504–514 (2019).
154. Wang, Y. *et al.* Heteroresistance Is Associated With in vitro Regrowth During Colistin Treatment in Carbapenem-Resistant *Klebsiella pneumoniae*. *Front. Microbiol.* **13**, (2022).
155. Ezadi, F., Ardebili, A. & Mirnejad, R. Antimicrobial Susceptibility Testing for Polymyxins: Challenges, Issues, and Recommendations. *J. Clin. Microbiol.* **57**, e01390-18 (2019).
156. Kim, J. W. & Lee, K. J. Single-nucleotide polymorphisms in a vancomycin-resistant *Staphylococcus aureus* strain based on whole-genome sequencing. *Arch. Microbiol.* **202**, 2255–2261 (2020).
157. Lamers, R. P., Cavallari, J. F. & Burrows, L. L. The efflux inhibitor phenylalanine-arginine beta-naphthylamide (PA β N) permeabilizes the outer membrane of gram-negative bacteria. *PloS One* **8**, e60666 (2013).